SEASONAL VARIATIONS OF THE MICROWAVE SCATTERING PROPERTIES OF THE DECIDUOUS TREES AS MEASURED IN THE 1-18 GHz SPECTRAL RANGE

Remote Sensing Laboratory

RSL Technical Report 177-60

T. Bush, F. Ulaby, T. Metzler, H. Stiles

Principal Investigator: Fawwaz T. Ulaby

June, 1976

Supported by:

NATIONAL AERONAUTICS AND SPACE ADMINISTRATION
Lyndon B. Johnson Space Center
Houston, Texas 77058

CONTRACT NAS 9-10261

THE UNIVERSITY OF KANSAS CENTER FOR RESEARCH, INC.
2291 Irving Hill Drive—Campus West Lawrence, Kansas 66045

THE UNIVERSITY OF KANSAS SPACE TECHNOLOGY CENTER
Raymond Nichols Hall Center for Research, Inc.
2291 Irving Hill Drive—Campus West Lawrence, Kansas 66045

Telephone: 913-864-4832

SEASONAL VARIATIONS OF THE MICROWAVE SCATTERING PROPERTIES OF DECIDUOUS TREES AS MEASURED IN THE 1-18 GHz SPECTRAL RANGE

Remote Sensing Laboratory

RSL Technical Report 177-60

T. Bush, F. Ulaby, T. Metzler, H. Stiles

Principal Investigator: Fawwaz T. Ulaby

June, 1976

Supported by: National Aeronautics and Space Administration
Lyndon B. Johnson Space Center
Houston, Texas 77058

CONTRACT NAS 9-10261

TABLE OF CONTENTS

LIST OF FIGURES

LIST OF FIGURES (CONTINUED)

ABSTRACT

Employing two FM-CW radar spectrometers, scattering data were acquired from stands of deciduous trees during the spring and autumn. The data suggest that the trees act as a volume scatter target particularly in the 7-18 GHz region. A comparison of data collected in spring and autumn indicates that the radar scattering coefficient, σ°, as measured in spring can be substantially larger (as much as 10 dB) than σ° as measured in the autumn.

1.0 INTRODUCTION

Of the earth's renewable natural resources forests are certainly one of the largest and one of the most versatile. Of the 13,034 million hectares of the earth's land mass approximately 4,126 million hectares, representing about 32 per cent, are forest covered [1]. Not only do these timberlands provide products such as fuel, building material and paper, they also provide recreational facilities and a host of benefits for the ecosystem such as wildlife habitat. Because of the sociological and ecological impact of possible mismanagement of these timberlands the management task has been assumed, to varying degrees, by most governments throughout the world.

Due to the vast areal extent of the world's forest covered land, relatively little quantitative information is available to the forest-land use manager. In many forested areas the nature of the terrain makes large scale surface surveys extremely difficult, if not prohibitively expensive. This is particularly true when repetitive collection of data is necessitated as is the case for annual identification and monitoring of clear-cut areas. Perhaps a more extreme example would be monthly assessment of forest fire damage. To alleviate the task of collecting the vast quantity of data needed to manage forest lands, forest managers have turned to the use of aerial photographic surveys. Indeed, of all the applications of remote sensing techniques, aerial photographic surveying of forest land is one of the best developed and best understood applications. This is not to say that photographic surveys are without limitations. Certainly photography cannot be employed to accurately make measurements of trunk diameter. Rather, as with nearly all remote sensing techniques, aerial photography is used to complement field work. (A well presented discussion of the applications and limitations of aerial photography to forest management is available from the U. S. Deparmtent of Agriculture [2]).

Because of the proven success of using photographic techniques in forest management it is a natural step to begin to investigate the possible benefits of applying other sensors to forest management. One possible candidate is side looking radar. Perhaps the most obvious difference between

radar imagery and photography is the vast difference in the wavelengths used in constructing the image. While photographic imagery is obtained using wavelengths on the order of microns, radar employs wavelengths on the order of centimeters. Because of this extreme difference in wavelength it is expected that radar imagery can provide information of a different nature than that provided through photographic techniques. A second important difference between photography and radar imagery is that radar can in general image much larger expanses of area than photographic techniques in a given amount of time. This can be an important advantage when timely information, such as the assessment of fire damage, is required. Radar has the added advantage of being able to penetrate cloud cover. This particular advantage and the ability of radar to quickly image large areas was clearly demonstrated by Project RAMP (Radar Mapping of Panama) in 1965 when the nearly continuously cloud covered Darien Province of Panama (17,000 km^2) was imaged in four hours [3].

While radar seems to have certain capabilities which may complement photographic techniques, these capabilities have not been thoroughly investigated. Indeed even in general terms very little qualitative data is available on the microwave scattering properties of woodlands. This report documents an experiment designed to aid in developing an understanding of the radar response to woodlands. Using two FM-CW radar spectrometers, scattering data were acquired from stands of mixed deciduous trees during the autumn, September 24, 1974 and during the spring, May 14, 1975.

2.0 INSTRUMENTATION

While the radar systems used in this experiment have been described elsewhere in detail [4,5], a brief description of these systems will be provided. Two systems, the MAS 1-8 (Microwave Active Spectrometer, 1-8 GHz) and the MAS 8-18 were employed to gather scattering data over the 1-18 GHz spectral range*. These are mobile, truck mounted FM-CW scatterometers employing hydraulic booms approximately 25 meters tall as instrumentation platforms. Both systems employ separate transmitting and receiving antennas

*Due to hardware difficulties data were not collected from 1-8 GHz during the autumn of 1974.

configured to allow both horizontal transmit-receive and vertical transmit-receive operation. During the winter months of 1975 both systems, the MAS 1-8 and the MAS 8-18, were fitted with improved antennas to allow cross (horizontal transmit, vertical receive) polarized operation during the springtime segment of the experiment. Measurements were acquired at 19 frequencies over the 1-18 GHz frequency range and at angles of incidence between 0° (nadir) and 80°. Table I summarizes the operational characteristics of the two scatterometers.

As noted in Table I, the RF bandwidths of the MAS 1-8 and the MAS 8-18 are 400 MHz and 800 MHz respectively. However, only a very small fraction of the bandwidth is used to provide range resolution which allows the majority of the bandwidth to be used for reducing signal scintillation. By assuming the envelope amplitude of the backscattered signal to be Rayleigh distributed it is possible to estimate the amount of signal variance reduction afforded by the excess bandwidth of the system [6]. This variance reduction is, however, directly proportional to D^{-1} where D is the extent of the illuminated target measured radially from the antenna. For a two dimensional target where little signal penetration can be expected, for example a very wet fallow field, D can be estimated rather accurately. However, when studying targets such as trees which will certainly allow a significant degree of signal penetration to occur, D cannot be accurately estimated. Thus it is rather difficult to assign specific confidence intervals (with respect to the reduction in scintillation variance) to the data presented herein. It should be noted, however, that spatial averaging was also employed by collecting scattering data at 15 different boom azimuth positions. Not only did this allow a further reduction in scintillation (over that provided by frequency averaging) but it also provided a better average of the scattering properties of the woodlands studied.

3.0 TARGET AREA DESCRIPTION

The wooded area studied during this experiment consisted of a rather typical northeastern Kansas distribution of hardwood trees located near Lawrence, Kansas. In particular the major varieties included in the area

TABLE 1.

MAS 1-8 and MAS 8-18 Nominal System Specifications

	MAS 1-8	MAS 8-18
TYPE	FM-CW	FM-CW
Modulating Waveform	Triangular	Triangular
Frequency Range	1-8 GHz	8-18 GHz
FM Sweep: Δf	400 MHz	800 MHz
Transmitter Power	10 dBm	10 dBm
Intermediate Frequency	50 KHz	50 KHz
IF Bandwidth	10 KHz	10 KHz
Antennas		
Height of ground	20 m	25 m
Reflector diameter	122 cm	46 cm
Feeds	Crossed Log-Periodic	Quad-Ridged Horn
Incidence Angle Range	0° (nadir)-80°	0° (nadir)-80°
Calibration:		
Internal	Signal Injection (delay line)	Signal Injection (delay line)
External	Luneberg Lens Reflector	Luneberg Lens Reflector

were elm, hickory, hackberry, and locust. Figure 1a through 1f are photographs of the test area taken with a camera boresighted with the antennas. As noted in the captions the photographs were taken at angles of incidence of 0°, 10°, 20°, 30°, 40° and 60°.

4.0 DATA PRESENTATION

4.1 Spectral Response of σ°

Figures 2 through 5 present the spectral response of σ_H° , σ_V° and σ_C° of the trees as measured during both the autumn and spring phases of the experiment (the subscript H, V and C refer to the polarization configuration). As noted earlier in this report no 1-8 GHz data were collected in the autumn nor were cross polarized measurements collected during the autumn. (Appendix A contains a listing of the data presented in this report). If we first consider Figure 2 in which the 0° (nadir) spectral response is plotted, a number of significant trends are apparent. The first observation is the consistent increasing trends of σ_H°,σ_V° (mostly between 1 and 10 GHz) and particularly σ_C° of the spring data. While σ_H° and σ_V° increase by about 2 dB and 5 dB respectively, σ_C° increases by approximately 11 dB as frequency is increased from 1-18 GHz. This is indeed suggestive of a target consisting of a random collection of scatterers whose geometric and dielectric properties become even more random and complex as the signal wavelength is decreased. Of equal significance is the difference in magnitude, approximately 3 dB to 5 dB, between those data collected in spring and autumn. Particularly noticeable is the vertically polarized data where a maximum difference of about 6 dB occurs at the higher frequencies.

In Figure 3, presenting the 20° data, these trends are even more apparent as noted by the 8 dB increases in σ_H° and σ_V° and the 10 dB increase in σ_C° as frequency is increased from 1-18 GHz. Perhaps of more interest, however, are the relative variations of the fall and spring data. While the spring data show a 4 dB increase as frequency increases from 8 to 18 GHz, the fall data remains relatively constant, or perhaps even decreases a small amount between 8 and 18 GHz. At the higher frequencies the fall and spring data exhibit a 10 dB separation, the spring data being the higher of the

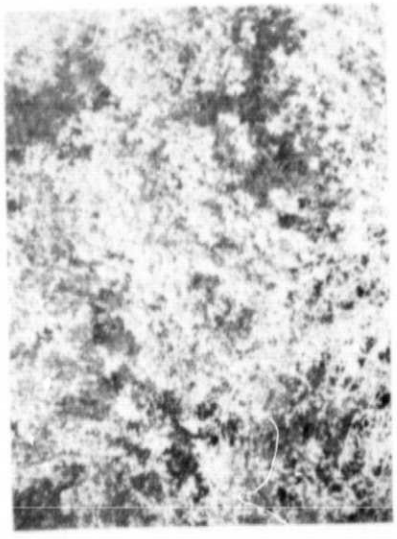

(a) 0°

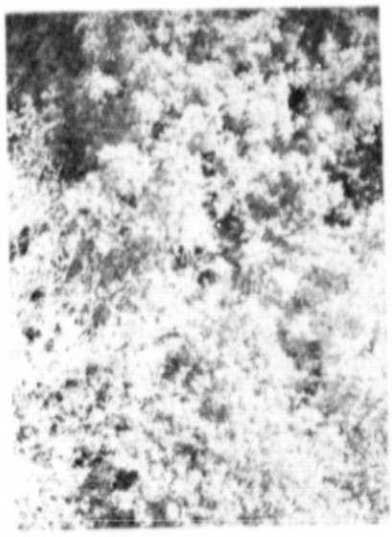

(b) 10°

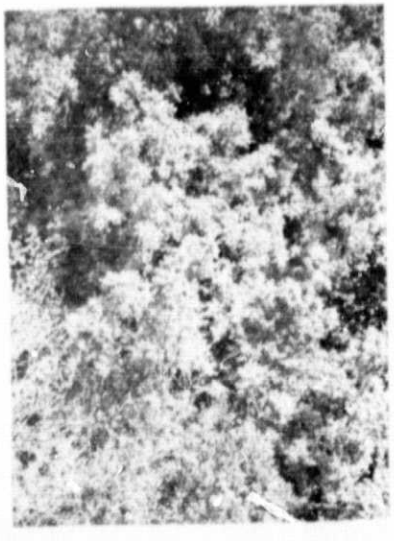

(c) 20°

(d) 30°

Figure 1. Photographs of Test Area as Taken with a Camera Boresighted with Antennas.

(e) 40°

(f) 60°

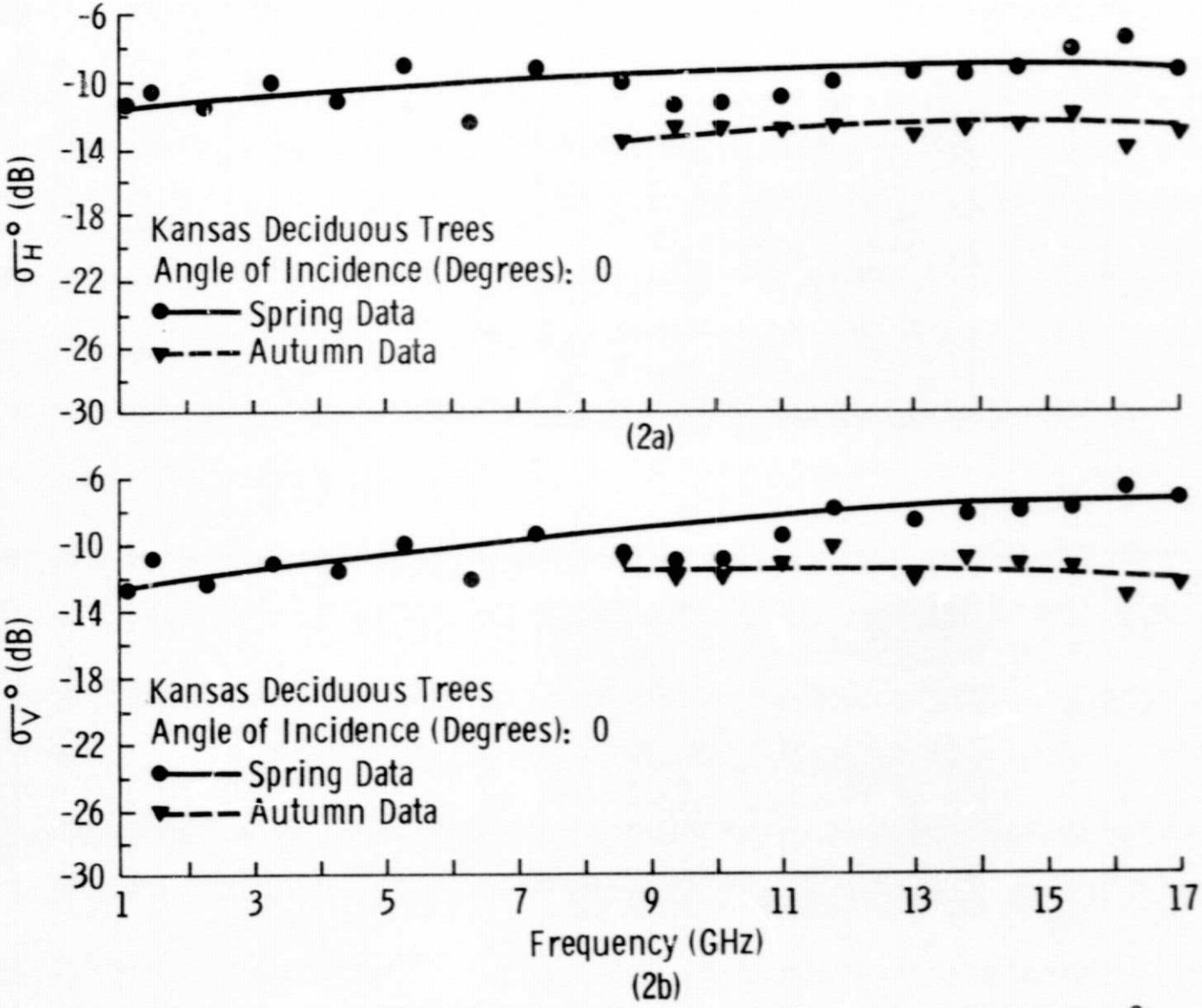

Figure 2. Spectral Responses of σ_H° (2a), σ_V° (2b), and σ_C° (2c) of Trees Measured at 0°.

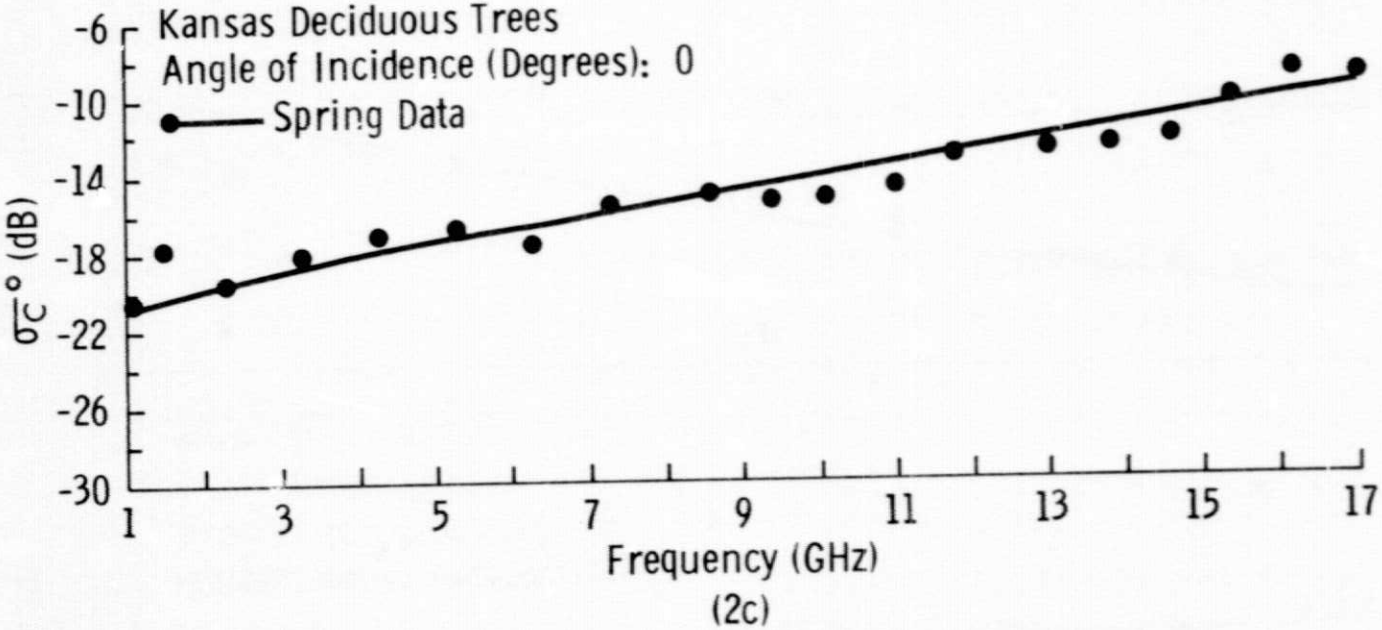
Kansas Deciduous Trees
Angle of Incidence (Degrees): 0
Spring Data
-6
-10
-14
-18
-22
-26
-30
$\overline{\sigma_c}°$ (dB)
1
3
5
7
9
11
13
15
17
Frequency (GHz)

(2c)

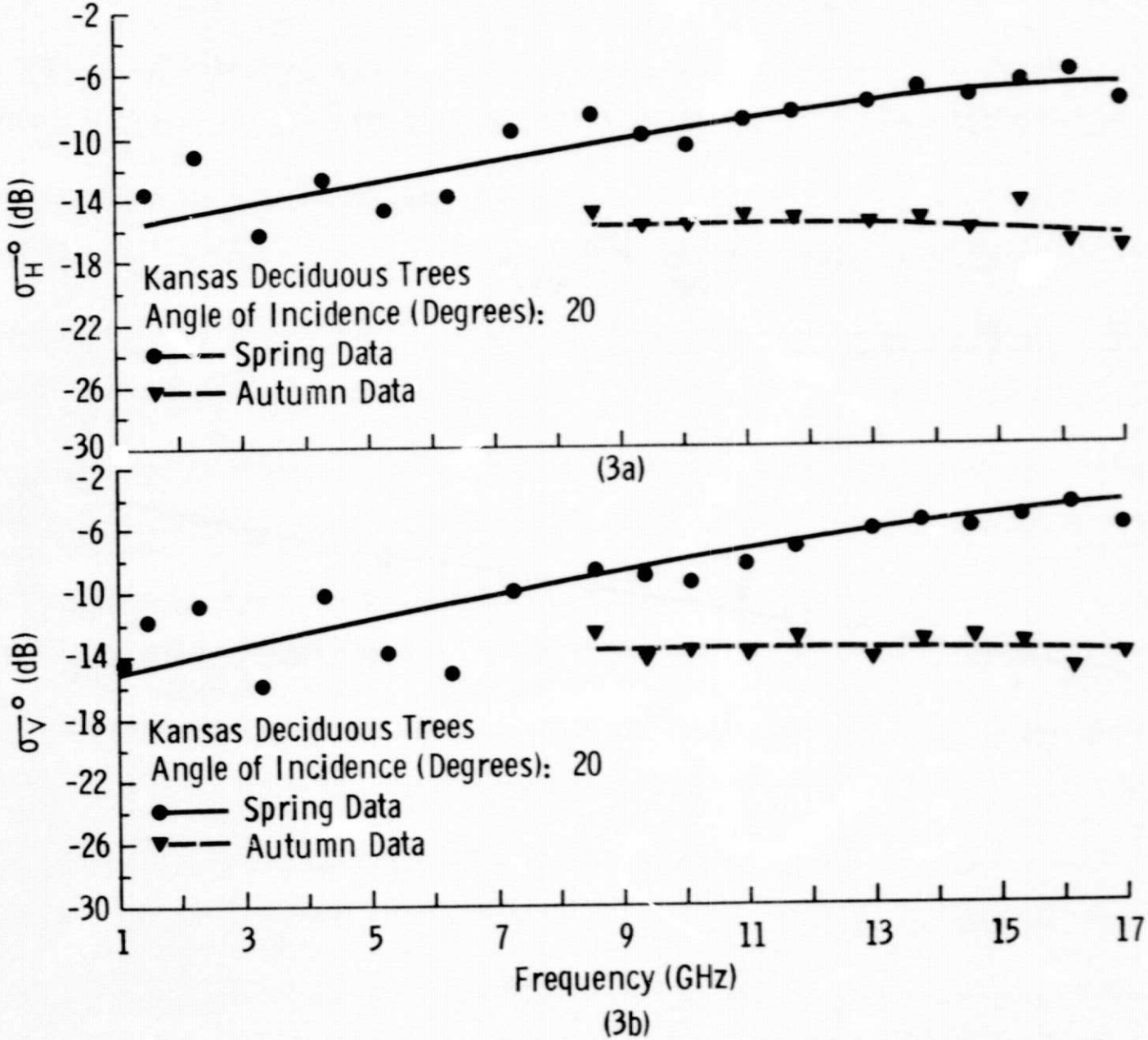

Figure 3. Spectral Responses of σ_H° (3a), σ_V° (3b), and σ_C° (3c) of Trees Measured at 20°.

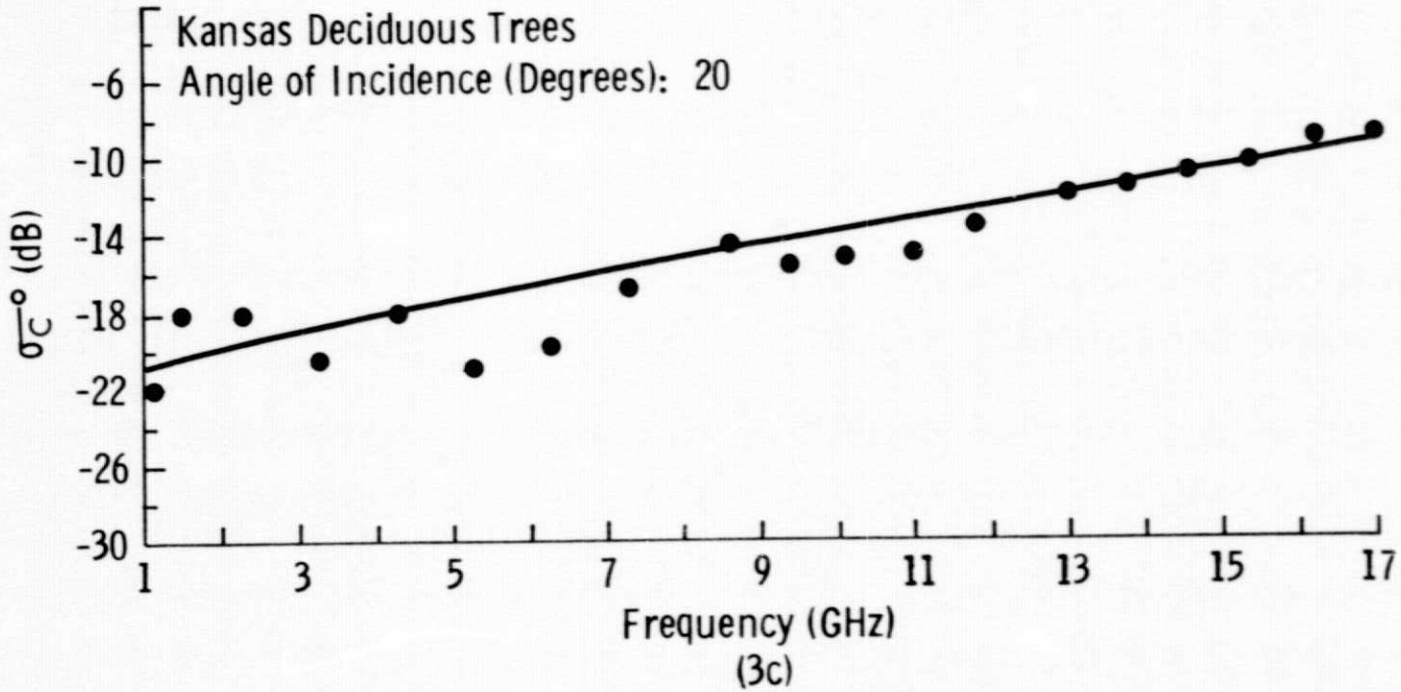
Kansas Deciduous Trees
Angle of Incidence (Degrees): 20
-6
-10
-14
-18
-22
-26
-30
σ_C° (dB)
1
3
5
7
9
11
13
15
17
Frequency (GHz)
(3c)

two. While the cause of this extreme difference in σ° for the autumn and spring data is not necessarily obvious, it is suggested that perhaps differing amounts of water contained in the leaves in spring and fall and the lesser density of leaves in the fall are probable causes.

Similar trends appear in the data collected at angles of incidence of 40° and 60°, Figures 4 and 5. At all angles the measurements from the spring phase of the experiment show a consistent increasing trend as frequency is varied from 1-18 GHz whereas the autumn gathered data exhibit a nearly frequency independent behavior in the 8-18 GHz portion of the spectrum. Furthermore the data collected during the autumn season were markedly lower than those data collected in the spring, particularly at the higher frequencies. Perhaps the most striking observation to be made, however, concerns the relative frequency variations of the like and cross polarized scattering coefficients. Note for example the relationship between σ_H° and σ_C° as measured at nadir as frequency increases from 1.0 GHz to 17.0 GHz. While the ratio $\sigma_C^\circ/\sigma_H^\circ$ at 1.0 GHz is -9.0 dB, $\sigma_C^\circ/\sigma_H^\circ$ at 17.0 GHz is +0.4 dB (Figure 6a).

The fact that σ_H° and σ_C° are nearly equal at the higher frequencies at nadir was quite troublesome at first notice. Data collected by Ament, MacDonald and Shewbridge [8] from New Jersey coniferous trees indicated for example that at nadir at a frequency of 9.3 GHz, $\sigma_{HV}^\circ/\sigma_{HH}^\circ = -12.5$ dB while the data reported herein indicate $\sigma_C^\circ/\sigma_H^\circ = -3.9$ dB at 9.4 GHz. However, a further inspection of the data reported by Ament et al. [8] shows that at L-band at 10° a ratio of $\sigma_{VH}^\circ/\sigma_{VV}^\circ = +1.3$ dB was measured while at 60° $\sigma_{VH}^\circ/\sigma_{VV}^\circ = +6.9$ dB.

Although it is felt that the rather large degree of depolarization measured is probably a result of dielectric anisotropy within the volume, a more exact explanation of this depolarization phenomenon cannot be suggested at this time. The same systems were used prior to and after this experiment to measure the backscatter of a Luneberg lens for calibration purposes and the backscatter of other vegetation types as part of other experiments, and in both cases the measured target depolarization was much smaller than was observed for the trees case. Hence it was concluded that the observed depolarization behavior can only be attributed to the trees and not to the system.

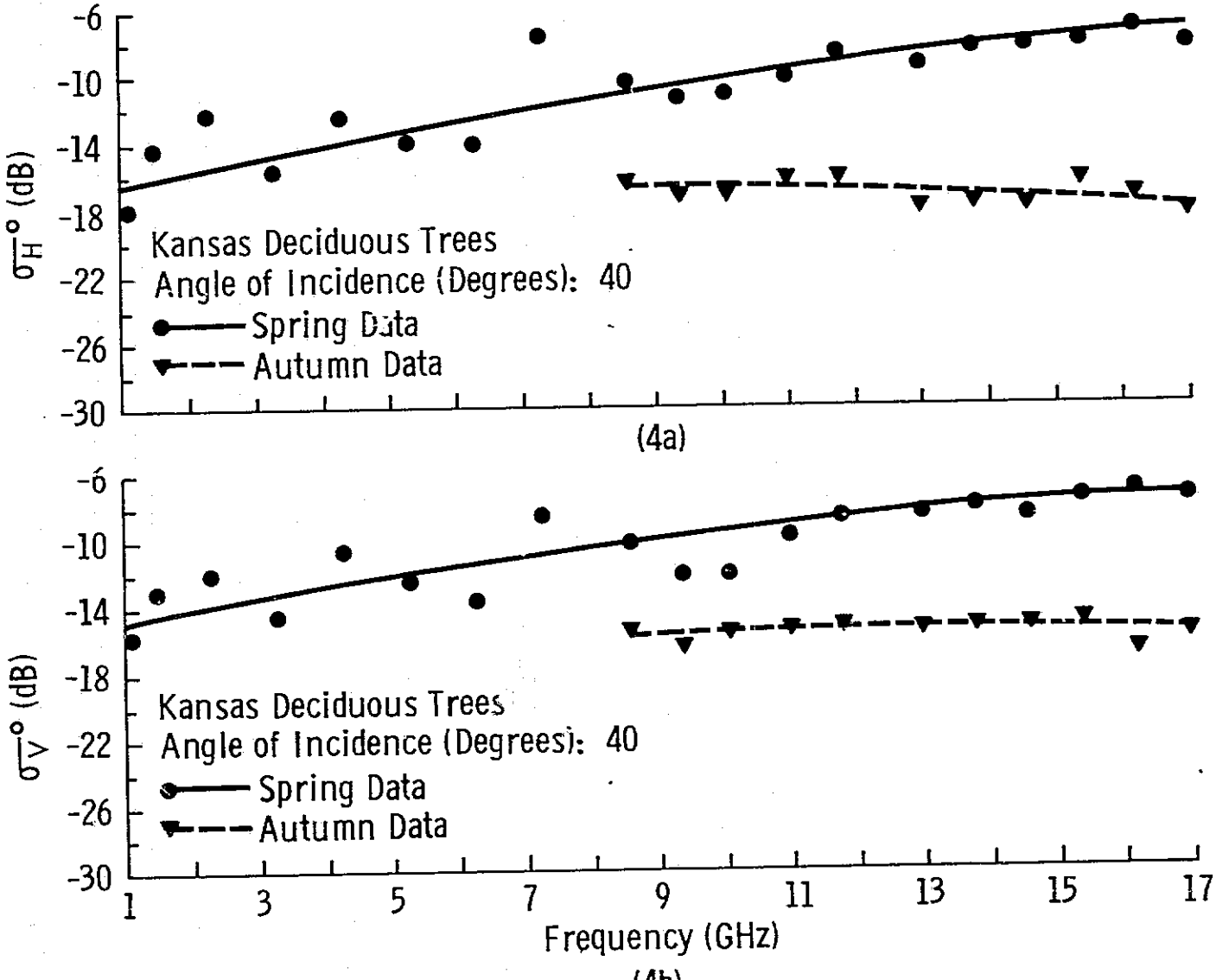

Figure 4. Spectral Responses of $\overline{\sigma_H}^\circ$ (4a), $\overline{\sigma_V}^\circ$ (4b), and $\overline{\sigma_C}^\circ$ (4c) of Trees Measured at 40°.

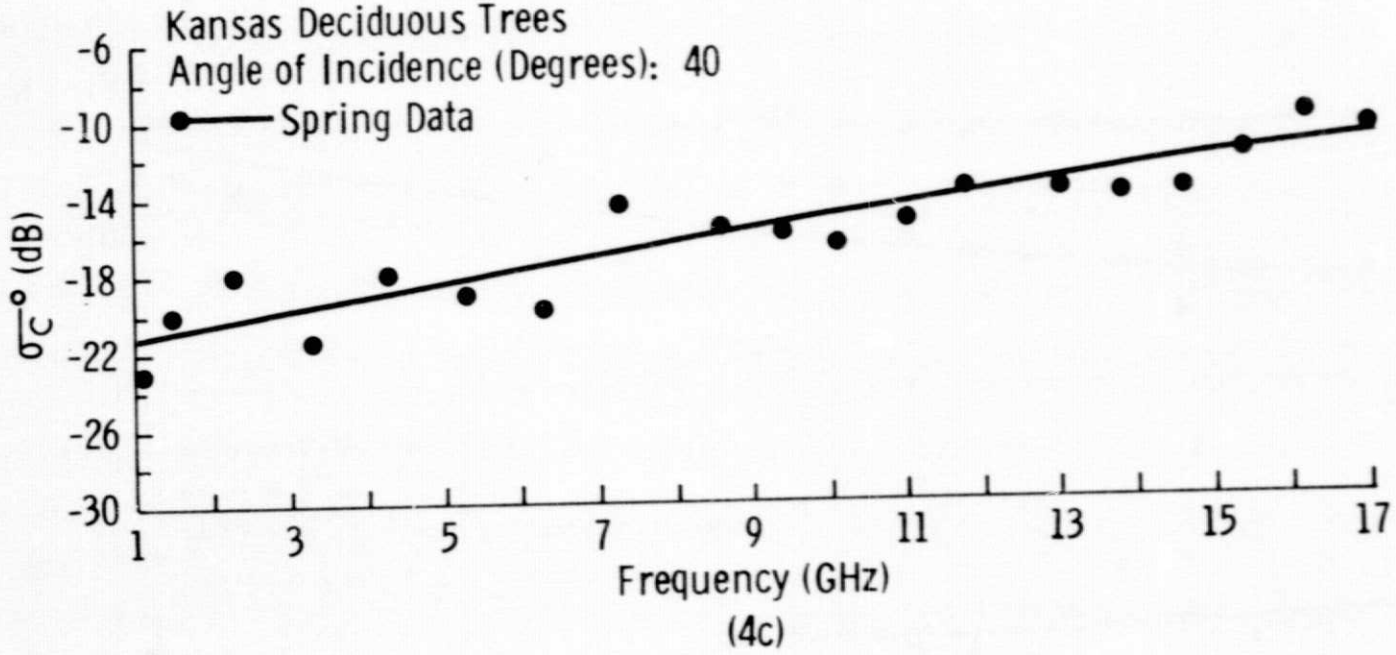
Kansas Deciduous Trees
Angle of Incidence (Degrees): 40
Spring Data
-6
-10
-14
-18
-22
-26
-30
σ_C° (dB)
1
3
5
7
9
11
13
15
17
Frequency (GHz)

(4c)

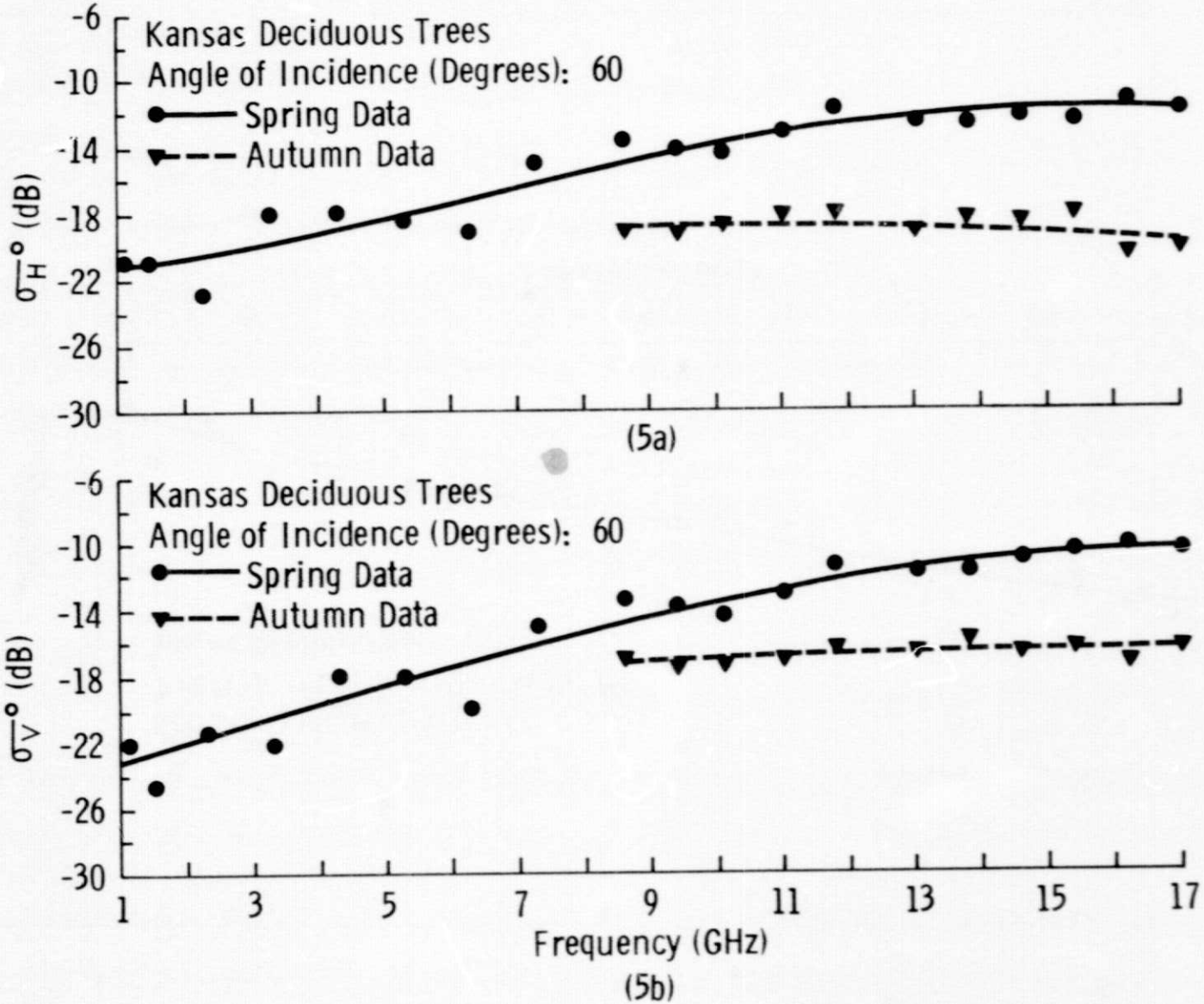

Figure 5. Spectral Responses of $\overline{\sigma_H}^\circ$ (5a), $\overline{\sigma_V}^\circ$ (5b), and $\overline{\sigma_C}^\circ$ (5c) of Trees Measured at 60°.

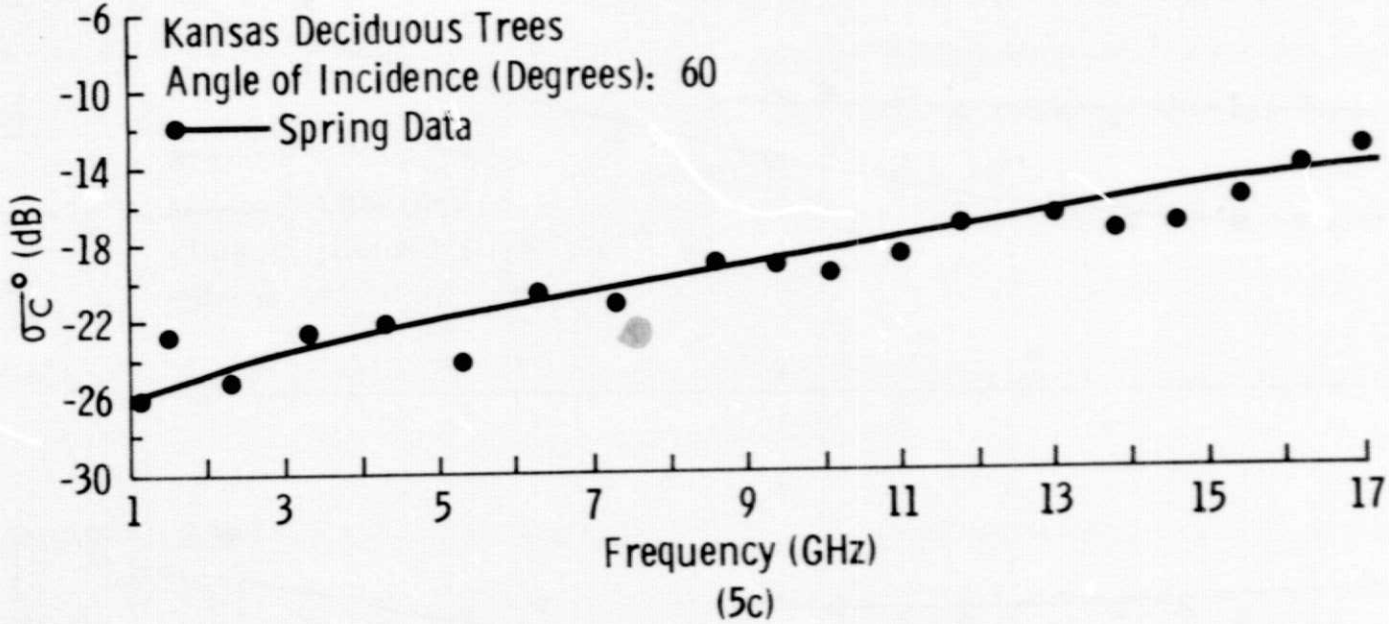
Kansas Deciduous Trees
Angle of Incidence (Degrees): 60
Spring Data
-6
-10
-14
-18
-22
-26
-30
σC° (dB)
1
3
5
7
9
11
13
15
17
Frequency (GHz)

(5c)

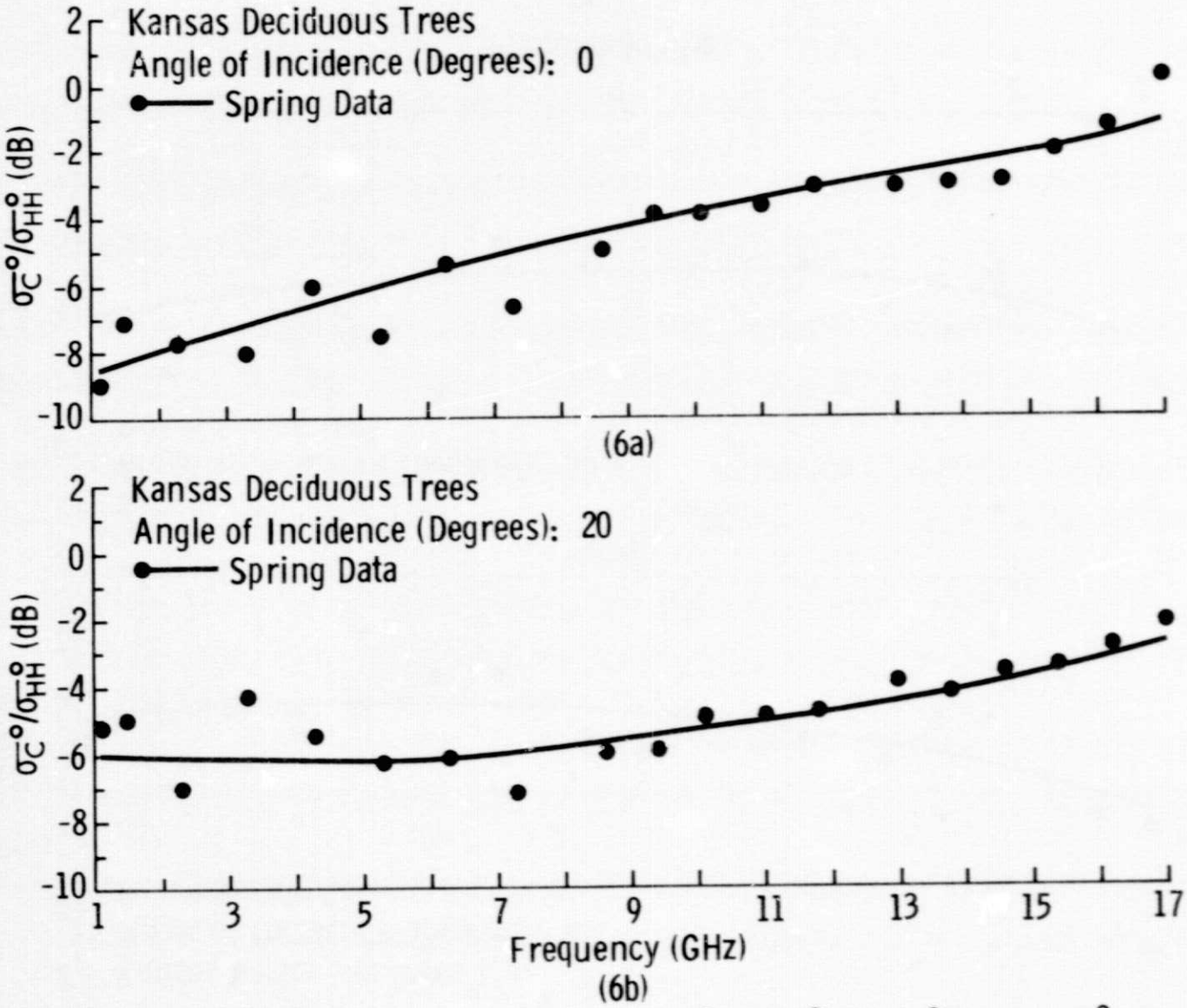

Figure 6. Spectral responses of $\sigma_C^\circ/\sigma_{HH}^\circ$(dB) at 0° (6a), 20° (6b), 40° (6c), and 60° (6d).

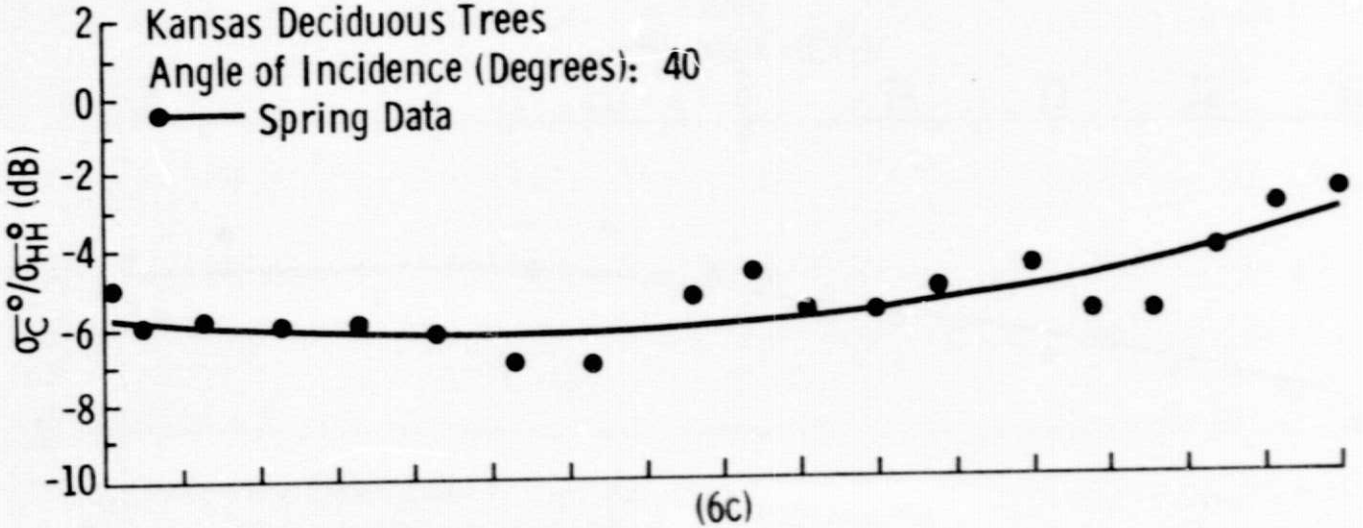
Kansas Deciduous Trees
Angle of Incidence (Degrees): 40
Spring Data
$\sigma_C^\circ/\sigma_{HH}^\circ$ (dB)
2
0
-2
-4
-6
-8
-10

(6c)

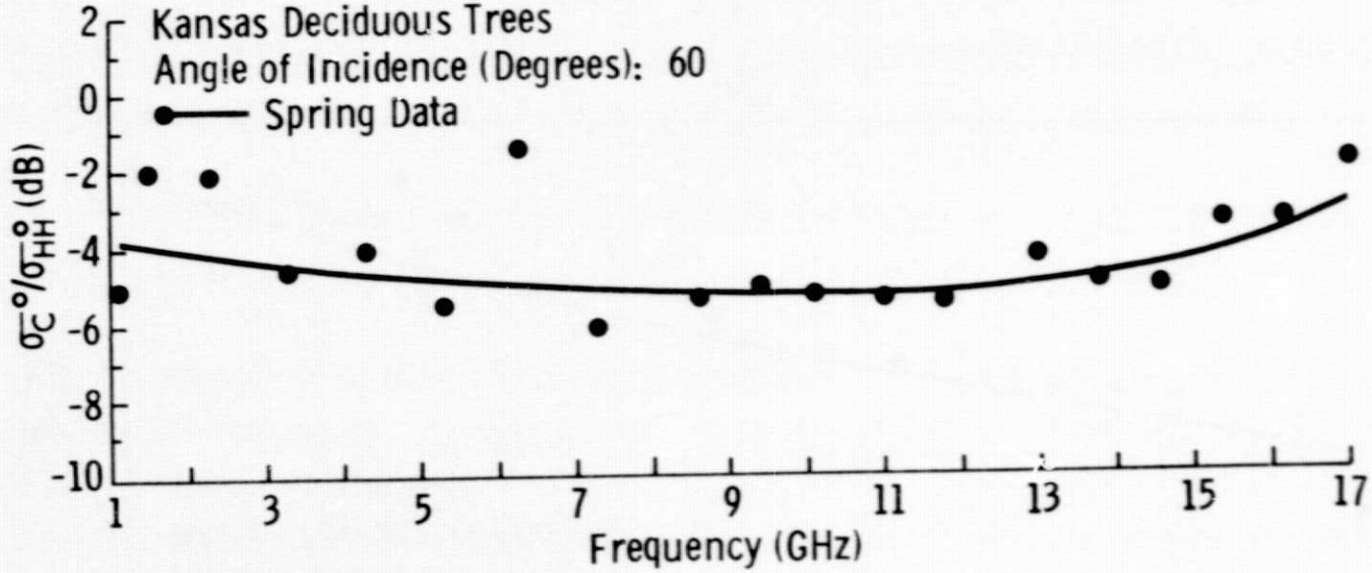
Kansas Deciduous Trees
Angle of Incidence (Degrees): 60
Spring Data
$\sigma_C^\circ/\sigma_{HH}^\circ$ (dB)
2
0
-2
-4
-6
-8
-10
1
3
5
7
9
11
13
15
17
Frequency (GHz)

(6d)

4.2 Angular Response of σ°

Because only 8-18 GHz data were collected both in the spring and autumn phases of the experiment, let us first compare the angular responses of the trees as measured between 8-18 GHz during these two differing seasons. Figure 7 presents σ_H° and σ_V° as measured at 8.6 GHz. Again the difference in magnitudes of σ° of the autumn and spring data is quite apparent, particularly in the 30° to 40° angular region. Furthermore there is a marked difference in the shapes of the two responses. The curve representing the spring data is again quite suggestive of a volume scattering phenomenon although the increasing trend of σ° between 0° and 10° is somewhat irregular for a volume effect. It is felt that this irregularity may be the result of the signal penetrating the tree canopy as viewed at nadir, thus introducing effects due to radar return from the soil surface. The autumn data also show the increase of σ° at the lower angles to a certain extent. Perhaps more surprising though is the relatively rapid decay in the autumn σ° curve between angles of incidence of 10° and 40°. Again it is suggested that the soil underlying the tree canopy is playing a role in determining the shape of these curves at the lower angles of incidence. This may be particularly true when considering the proposition that during the autumn phase of the experiment the leaves were less dense and held considerably less moisture than during the spring phase. At angles of incidence greater than 40° the autumn data remains fairly constant while the spring data continues to decay.

At 13.0 GHz, Figure 8, the trends are similar to those noted at 8.6 GHz. At this higher frequency, however, the separation between the spring and autumn data is quite extreme, nearly 9 dB for σ_H° at 30° and about 8 dB for σ_V° at 30°. Finally at 17.0 GHz, Figure 9, the separation, at 30°, between the autumn and springtime data has reached about 10-12 dB. The trends of the data have remained, in general, very similar throughout the frequency range from 8-18 GHz.

Next let us compare the angular response of all three polarizations, HH, VV and cross between 1 and 18 GHz for the spring data. In Figures 10 through 15 both σ° and γ are plotted where $\gamma = \sigma^\circ/\cos\theta$ (θ is the angle of incidence). Consider Figures 10a and 10b containing 1.1 GHz data. Note that in these figures the angular responses do not immediately suggest that a

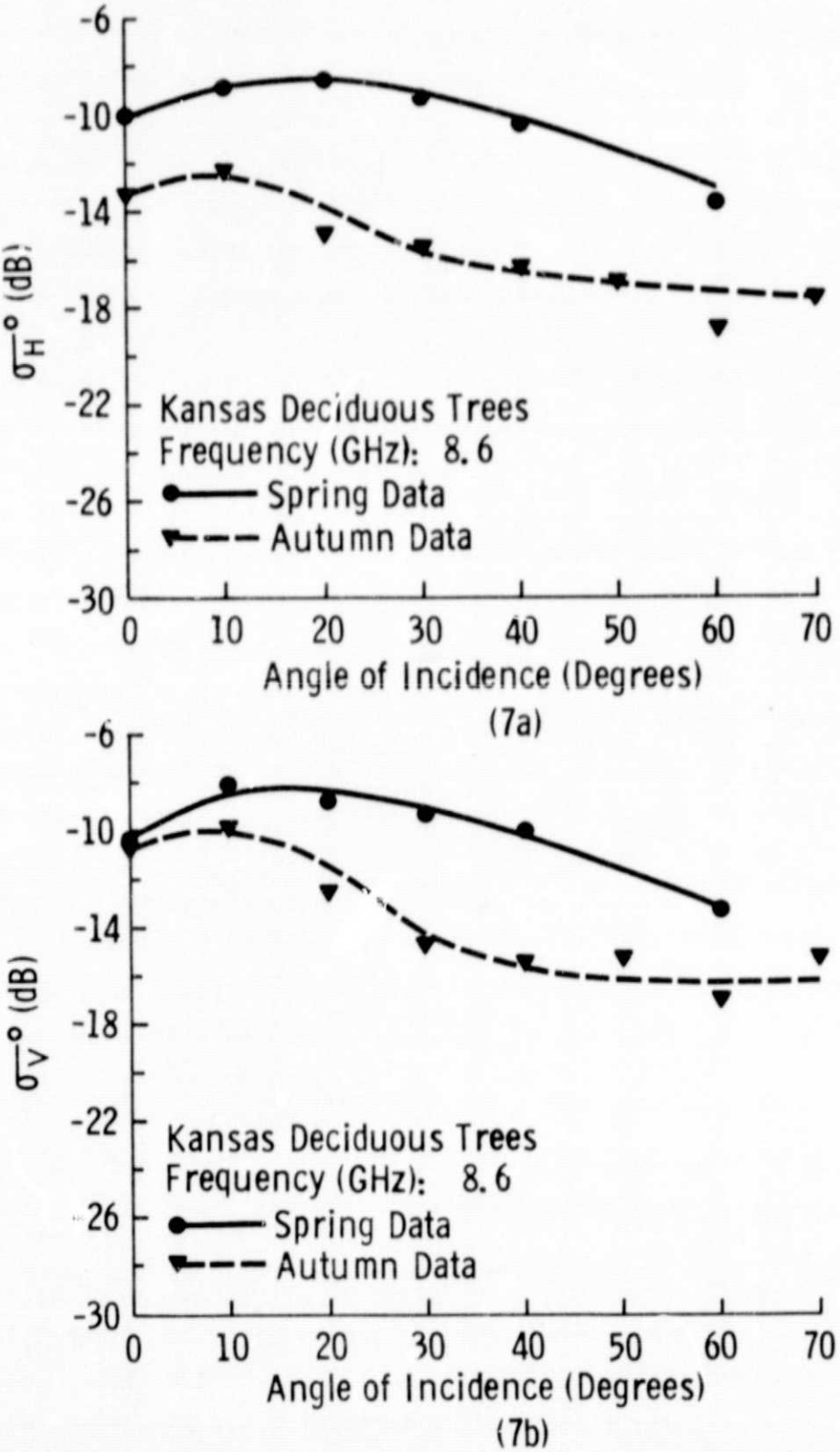

Figure 7. Angular Variations of $\overline{\sigma_H}^\circ$ (7a) and $\overline{\sigma_V}^\circ$ (7b) of Trees Measured at 8.6 GHz in the Spring and Autumn.

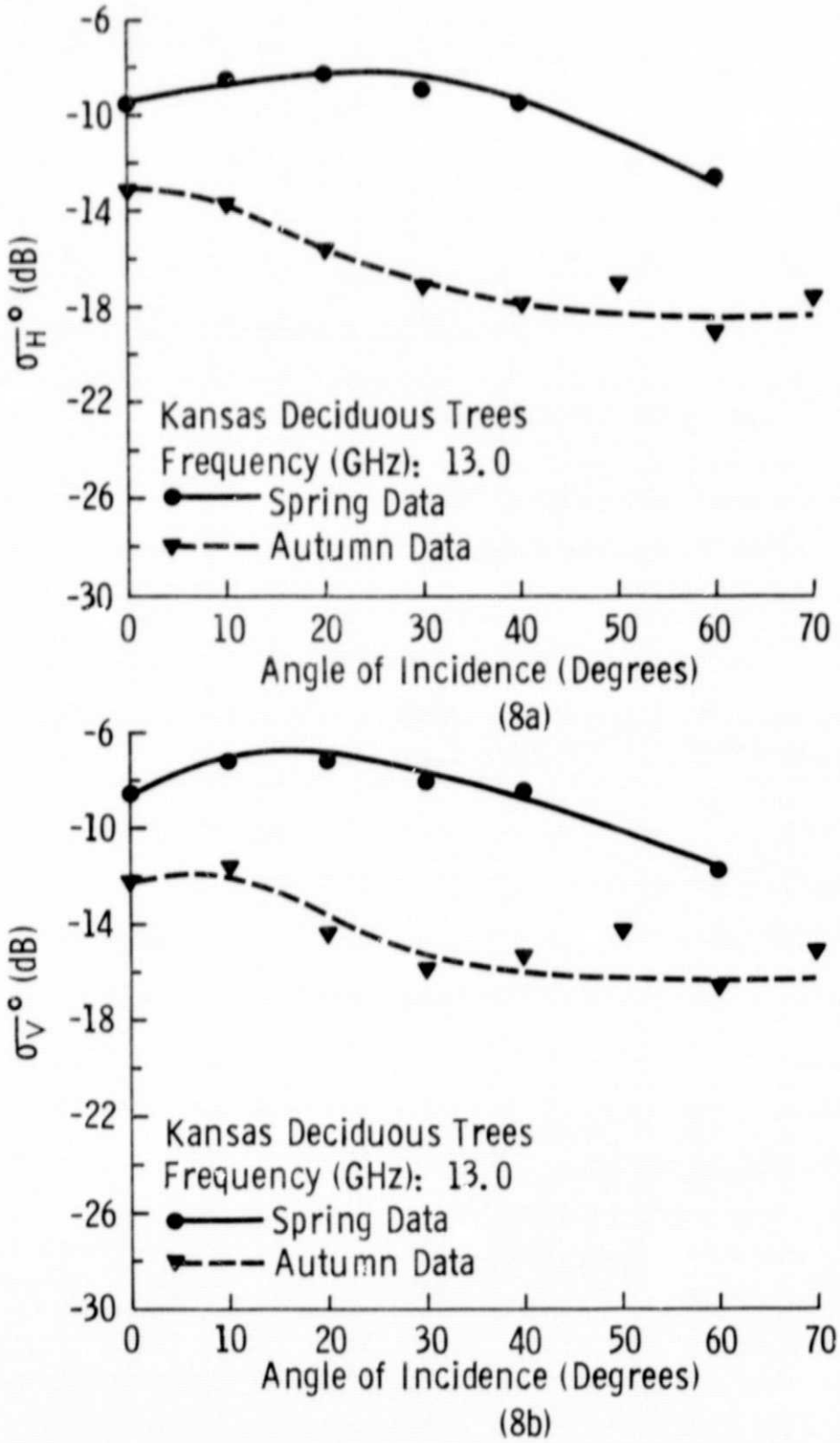

Figure 8. Angular Variations of $\overline{\sigma_H}^\circ$ (8a) and $\overline{\sigma_V}^\circ$ (8b) of Trees Measured at 13.0 GHz in the Spring and Autumn.

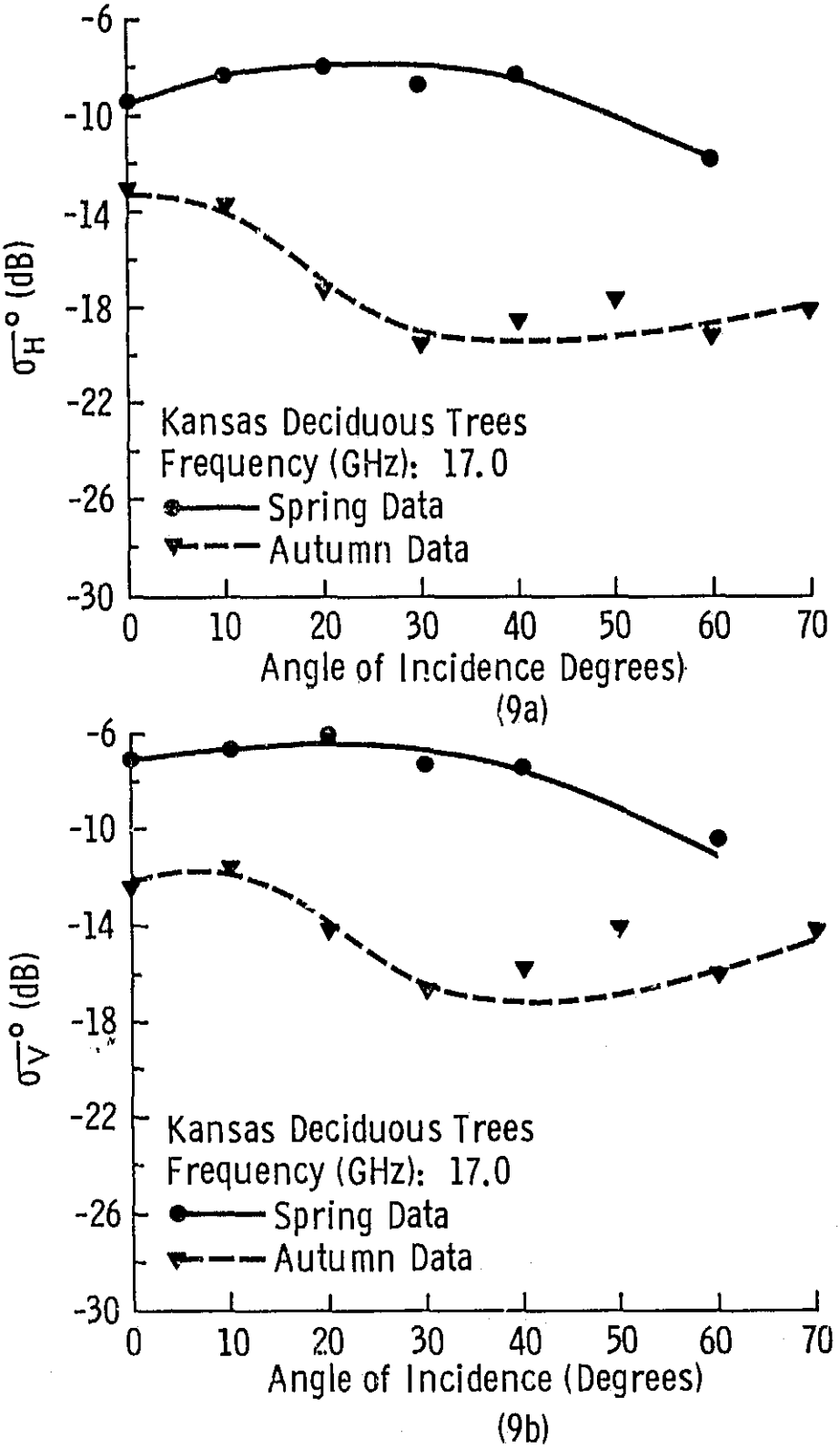

Figure 9. Angular Variations of $\overline{\sigma_H}^\circ$ (9a) and $\overline{\sigma_V}^\circ$ (9b) of Trees Measured at 17.0 GHz in the Spring and Autumn.

AVERAGED SIGMA0 SPRING, 1975

ANTENNA ANGLE 0

FREQ	8.6	9.4	10.2	11.0	11.8	13.0	13.8	14.6	15.4	16.2	17.0
POL HH	-10.0	-11.4	-11.3	-10.9	-10.0	-9.5	-9.6	-9.3	-8.2	-7.5	-9.4
POL HV	-15.0	-15.3	-15.2	-14.6	-13.1	-12.7	-12.6	-12.3	-10.3	-8.8	-9.0
POL VV	-10.5	-11.0	-10.9	-9.6	-7.9	-8.6	-8.2	-8.0	-7.7	-6.5	-7.2

ANTENNA ANGLE 10

FREQ	8.6	9.4	10.2	11.0	11.8	13.0	13.8	14.6	15.4	16.2	17.0
POL HH	-8.9	-10.8	-10.4	-9.7	-9.5	-8.5	-8.0	-7.7	-7.3	-7.0	-8.3
POL HV	-14.9	-14.8	-15.8	-14.7	-13.1	-12.4	-12.7	-12.0	-10.0	-9.5	-9.2
POL VV	-8.1	-9.0	-9.5	-8.6	-7.7	-7.2	-7.5	-7.4	-6.9	-6.3	-6.8

ANTENNA ANGLE 20

FREQ	8.6	9.4	10.2	11.0	11.8	13.0	13.8	14.6	15.4	16.2	17.0
POL HH	-8.6	-9.7	-10.4	-9.1	-8.7	-8.2	-7.3	-7.7	-6.9	-6.2	-7.9
POL HV	-14.5	-15.6	-15.3	-15.0	-13.5	-12.0	-11.6	-11.2	-10.3	-9.0	-9.0
POL VV	-8.8	-8.9	-9.4	-8.4	-7.5	-7.2	-6.7	-7.2	-6.4	-5.6	-6.2

ANTENNA ANGLE 30

FREQ	8.6	9.4	10.2	11.0	11.8	13.0	13.8	14.6	15.4	16.2	17.0
POL HH	-9.3	-10.7	-10.9	-10.2	-8.2	-8.8	-8.7	-8.3	-8.2	-7.5	-9.7
POL HV	-15.1	-13.2	-16.0	-15.1	-13.8	-12.9	-13.3	-13.0	-11.6	-10.3	-11.1
POL VV	-9.3	-9.8	-9.6	-9.6	-7.8	-8.1	-8.3	-7.9	-7.5	-7.0	-7.4

ANTENNA ANGLE 40

FREQ	8.6	9.4	10.2	11.0	11.8	13.0	13.8	14.6	15.4	16.2	17.0
POL HH	-10.4	-11.4	-11.2	-10.2	-8.7	-9.4	-8.5	-8.3	-8.1	-7.2	-8.3
POL HV	-15.7	-16.0	-16.7	-15.4	-13.8	-13.9	-14.2	-14.0	-12.2	-10.3	-10.9
POL VV	-10.1	-11.0	-11.0	-9.7	-8.6	-8.5	-8.2	-8.7	-7.6	-7.2	-7.5

ANTENNA ANGLE 60

FREQ	8.6	9.4	10.2	11.0	11.8	13.0	13.8	14.6	15.4	16.2	17.0
POL HH	-13.7	-14.3	-14.5	-13.3	-11.8	-12.6	-12.7	-12.3	-12.5	-11.3	-11.8
POL HV	-19.1	-19.4	-19.8	-18.8	-17.3	-16.9	-17.7	-17.4	-16.0	-14.5	-13.5
POL VV	-13.5	-13.9	-14.5	-13.2	-11.5	-11.8	-11.8	-11.1	-10.6	-10.3	-10.6

AVERAGED SIGMAO FALL, 1974

ANTENNA ANGLE 0

FREQ	8.6	9.4	10.2	11.0	11.8	13.0	13.8	14.6	15.4	16.2	17.0
POL HH	-13.4	-12.6	-12.7	-12.7	-12.5	-13.2	-12.8	-12.5	-11.9	-14.0	-13.0
POL HV	0.	0.	0.	0.	0.	0.	0.	0.	0.	0.	0.
POL VV	-10.8	-12.0	-11.9	-11.2	-10.2	-12.1	-10.8	-11.2	-11.4	-13.2	-12.4

ANTENNA ANGLE 10

FREQ	8.6	9.4	10.2	11.0	11.8	13.0	13.8	14.6	15.4	16.2	17.0
POL HH	-12.3	-12.6	-11.8	-12.2	-13.0	-13.7	-12.0	-12.3	-11.1	-13.3	-13.8
POL HV	0.	0.	0.	0.	0.	0.	0.	0.	0.	0.	0.
POL VV	-9.8	-11.2	-10.6	-11.4	-10.8	-11.6	-9.8	-10.7	-10.7	-12.5	-11.6

ANTENNA ANGLE 20

FREQ	8.6	9.4	10.2	11.0	11.8	13.0	13.8	14.6	15.4	16.2	17.0
POL HH	-14.9	-15.7	-15.7	-15.1	-15.4	-15.7	-15.3	-16.2	-14.4	-17.2	-17.3
POL HV	0.	0.	0.	0.	0.	0.	0.	0.	0.	0.	0.
POL VV	-12.5	-14.3	-13.8	-14.1	-13.2	-14.4	-13.3	-13.2	-13.5	-15.3	-14.2

ANTENNA ANGLE 30

FREQ	8.6	9.4	10.2	11.0	11.8	13.0	13.8	14.6	15.4	16.2	17.0
POL HH	-15.5	-16.7	-16.3	-16.1	-16.4	-17.2	-17.6	-17.9	-16.7	-19.3	-19.5
POL HV	0.	0.	0.	0.	0.	0.	0.	0.	0.	0.	0.
POL VV	-14.7	-16.5	-15.6	-15.8	-15.4	-15.9	-15.6	-15.7	-15.2	-17.6	-16.7

ANTENNA ANGLE 40

FREQ	8.6	9.4	10.2	11.0	11.8	13.0	13.8	14.6	15.4	16.2	17.0
POL HH	-16.3	-17.3	-17.2	-16.2	-16.2	-17.9	-17.8	-17.8	-16.3	-17.3	-18.4
POL HV	0.	0.	0.	0.	0.	0.	0.	0.	0.	0.	0.
POL VV	-15.4	-16.4	-15.5	-15.3	-15.2	-15.3	-15.2	-15.1	-14.9	-16.7	-15.8

ANTENNA ANGLE 50

FREQ	8.6	9.4	10.2	11.0	11.8	13.0	13.8	14.6	15.4	16.2	17.0
POL HH	-17.0	-17.5	-17.3	-16.6	-16.2	-17.1	-16.5	-15.8	-15.2	-17.2	-17.6
POL HV	0.	0.	0.	0.	0.	0.	0.	0.	0.	0.	0.
POL VV	-15.2	-15.6	-15.4	-14.4	-13.9	-14.4	-14.1	-13.3	-13.4	-15.4	-14.2

ANTENNA ANGLE 60

FREQ	8.6	9.4	10.2	11.0	11.8	13.0	13.8	14.6	15.4	16.2	17.0
POL HH	-19.0	-19.3	-18.8	-18.1	-18.0	-19.1	-18.5	-18.6	-18.0	-19.4	-19.2
POL HV	0.	0.	0.	0.	0.	0.	0.	0.	0.	0.	0.
POL VV	-17.0	-17.6	-17.4	-17.1	-16.4	-16.6	-15.8	-16.7	-16.4	-17.4	-16.1

ANTENNA ANGLE 70

FREQ	8.6	9.4	10.2	11.0	11.8	13.0	13.8	14.6	15.4	16.2	17.0
POL HH	-17.6	-17.6	-17.3	-16.7	-16.6	-17.6	-17.2	-16.2	-15.7	-17.7	-18.1
POL HV	0.	0.	0.	0.	0.	0.	0.	0.	0.	0.	0.
POL VV	-15.1	-16.2	-14.8	-15.2	-14.4	-15.2	-14.1	-13.8	-14.1	-16.1	-14.2

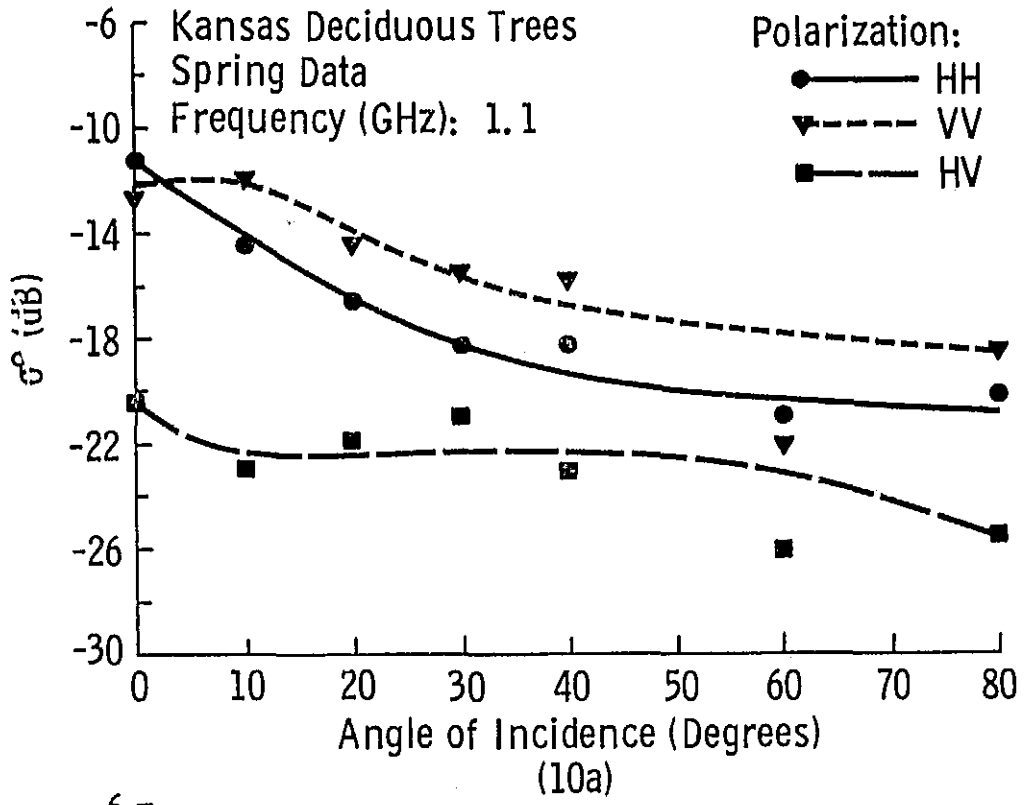

(10a)

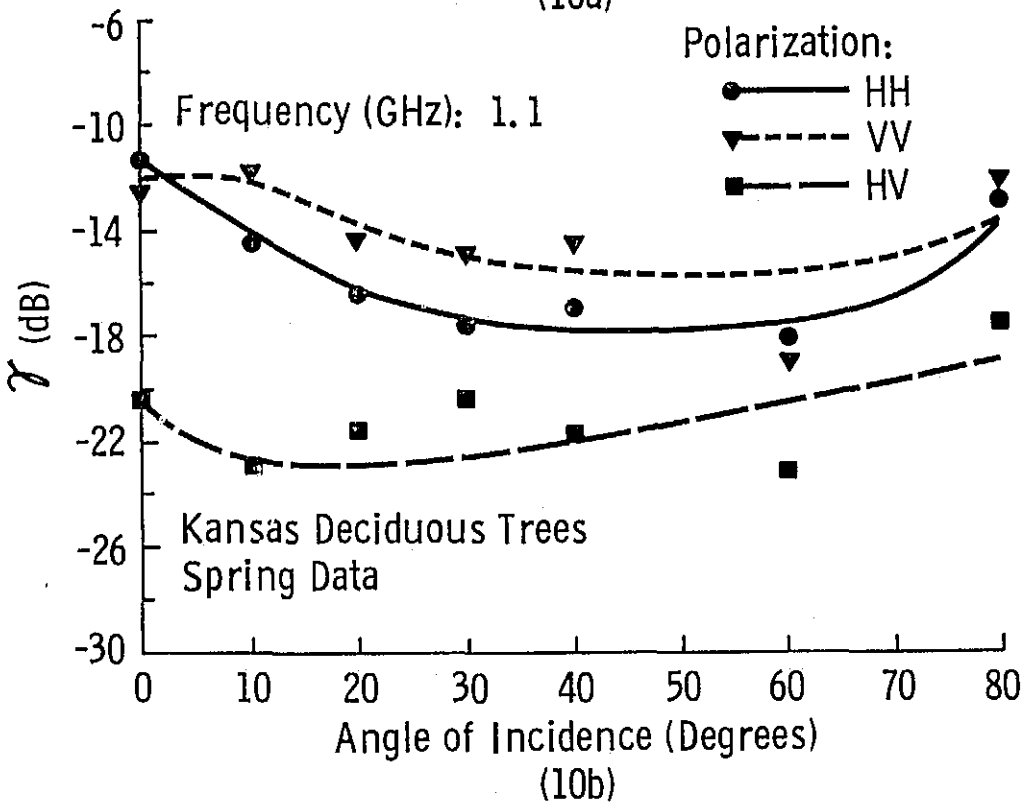

(10b)

Figure 10. Angular Variations of $\overline{\sigma_H}^o$, $\overline{\sigma_V}^o$, and $\overline{\sigma_C}^o$ (10a) and γ_H, γ_V, and γ_C (10b) as Measured at 1.1 GHz. The Data Depicted in This Figure Were Gathered in Springtime.

volume scatter phenomenon is dominant. Certainly the target does not appear extremely smooth but σ_H° does show a 7 dB decay between 0° and 30°. Also, while σ_H° and σ_V° show similar returns at nadir, the shapes of the curves are somewhat different with σ_H° being lower than σ_V° at all angles but nadir. σ_C° shows a very flat response between 0° and 50° at which point the σ_C° begins to decay. Expressed as γ , Figure 10b, the curves have a tendency to show an increase in magnitude at the higher angles.

At 3.3 GHz, Figure 11, σ_H° and σ_V° have more similar responses than those at 1.1 GHz. σ_H° and σ_V° begin to show an indication that volume scatter is becoming more pronounced. Except at nadir (at which angle it is felt that return from the soil is significant) the curves of σ° are relatively flat between 10° and 40° at which point a slow decay begins. As at 1.1 GHz, σ_C° shows a very flat response between 10° and 60°. In Figure 11b, γ has a flatter response than at 1.1 GHz although the tendency for γ to increase at the higher angles is still apparent.

At 7.3 GHz, Figures 12a and 12b, it is noted that volume scatter is becoming quite prominent. Note the nearly identical response of σ_H° and σ_V° and that the curves of σ° show a trend characteristic of a volume scatter phenomenon. σ_C° shows a response similar to σ_H° and σ_V°. Note that γ_H and γ_V, Figure 12b, exhibits a nearly flat response between 0° and 60° with γ_C showing a dip in magnitude at 10°.

Next consider the angular response of σ° and γ at 8.6 GHz as plotted in Figures 13a and 13b. For all practical purposes, the horizontally and vertically polarized returns are identical. Note also that the cross polarized return, while about 6 dB lower than the like polarized returns, has very nearly an identical shape as the like polarized returns. Furthermore as shown in Figure 13b, γ has a fairly flat response throughout the 0° to 80° angular range.

In Figures 14 and 15 the angular responses of the 13.0 and 17.0 GHz data continue to indicate that volume scatter is predominant. At both frequencies the horizontally and vertically polarized returns show very similar responses as a function of angle of incidence. The cross polarized returns, while similar in shape to the like polarized returns, show a tendency to increase in magnitude as frequency is increased. Moreover γ , at both 13.0 and 17.0 GHz shows an almost flat response throughout the angular range.

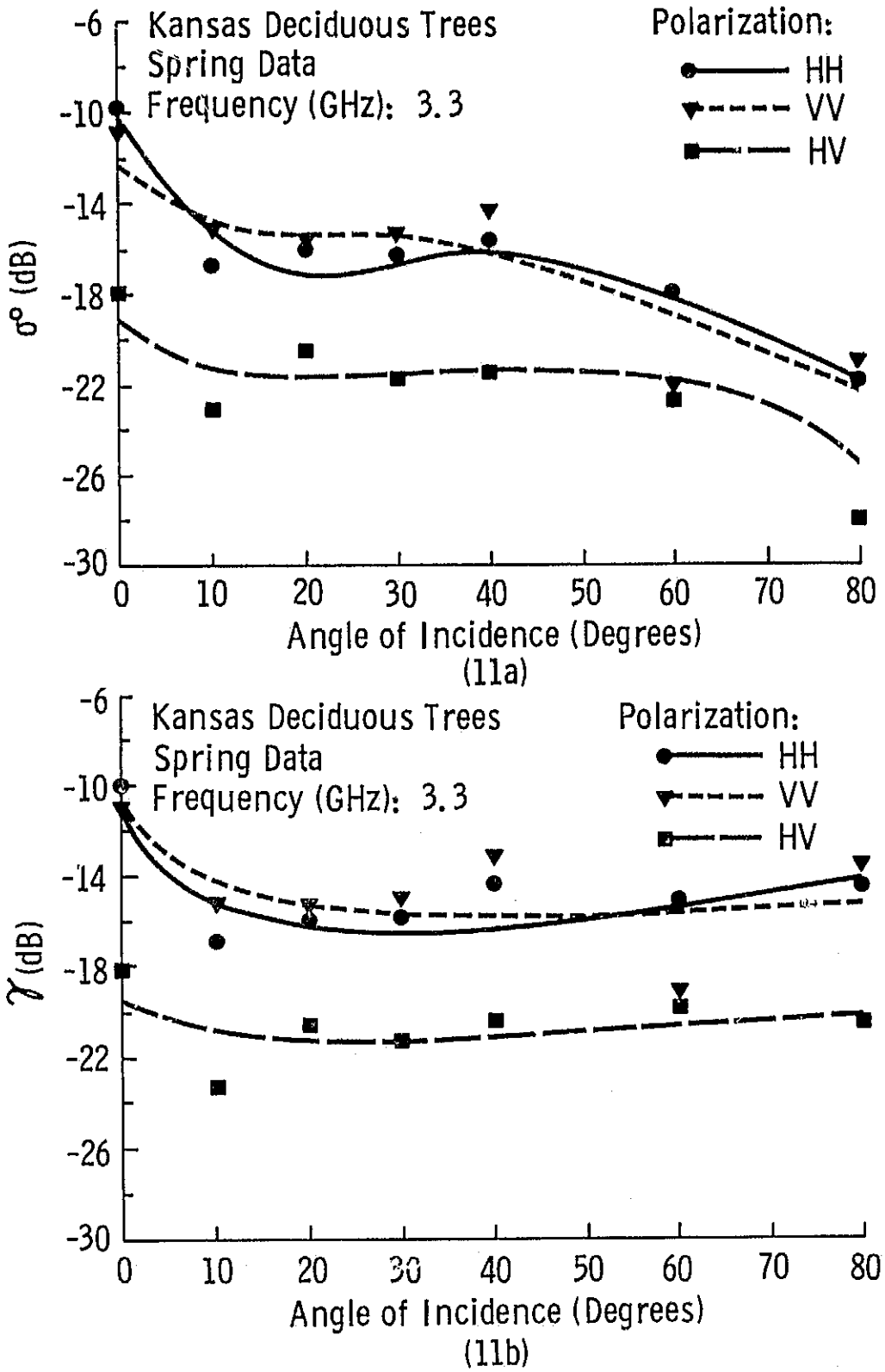

Figure 11. Angular Variations of $\overline{\sigma_H}^\circ$, $\overline{\sigma_V}^\circ$, and $\overline{\sigma_C}^\circ$ (11a) and γ_H, γ_V, and γ_C (11b) as Measured at 3.3 GHz. The Data Depicted in This Figure Were Gathered in Springtime.

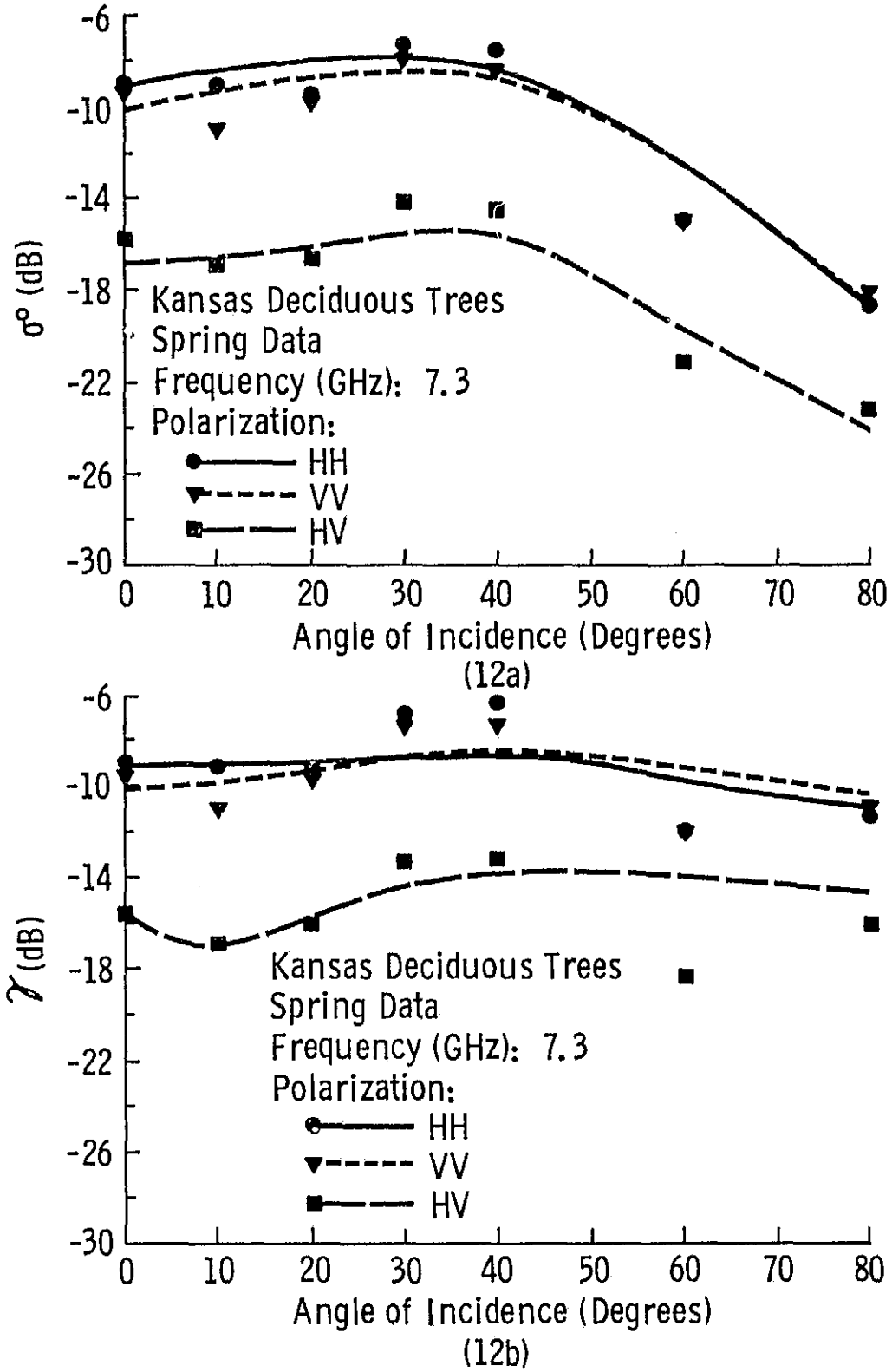

Figure 12. Angular Variations of $\overline{\sigma_H}^{\circ}$, $\overline{\sigma_V}^{\circ}$, and $\overline{\sigma_C}^{\circ}$ (12a) and γ_H, γ_V, and γ_C (12b) as Measured at 7.3 GHz. The Data Depicted in This Figure Were Gathered in the Springtime.

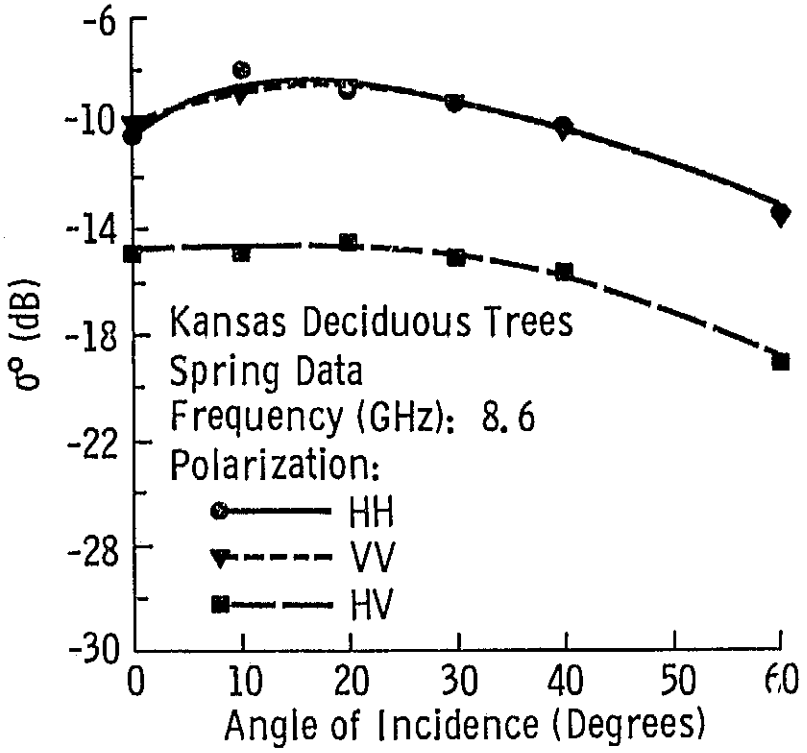

(13a)

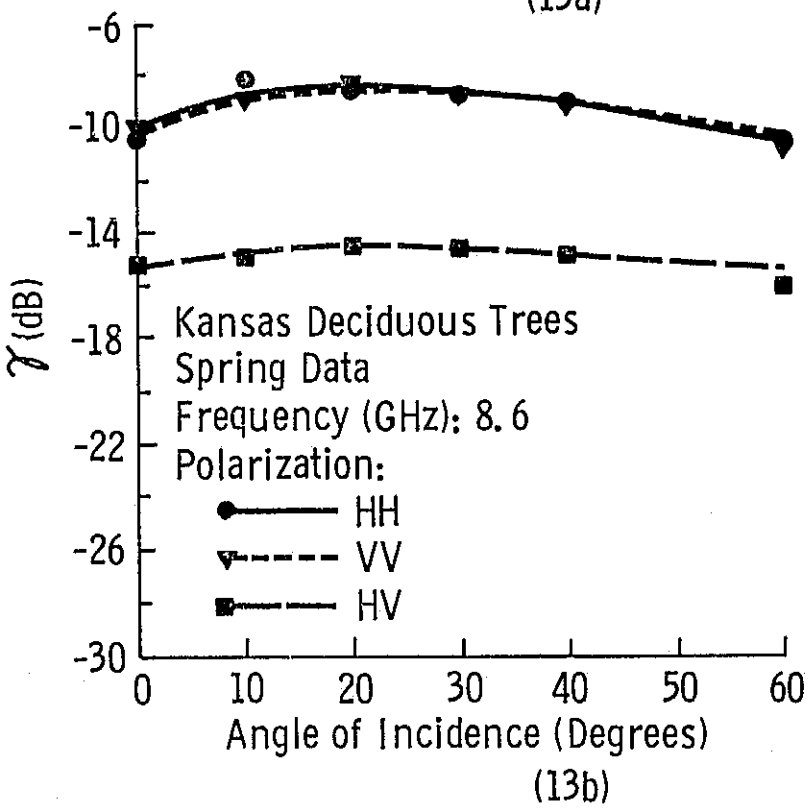

(13b)

Figure 13. Angular Variations of $\overline{\sigma_H}^\circ$, $\overline{\sigma_V}^\circ$, and $\overline{\sigma_C}^\circ$ (13a) and γ_H, γ_V, and γ_C (13b) as Measured at 8.6 GHz. The Data Depicted in This Figure Were Gathered in the Springtime.

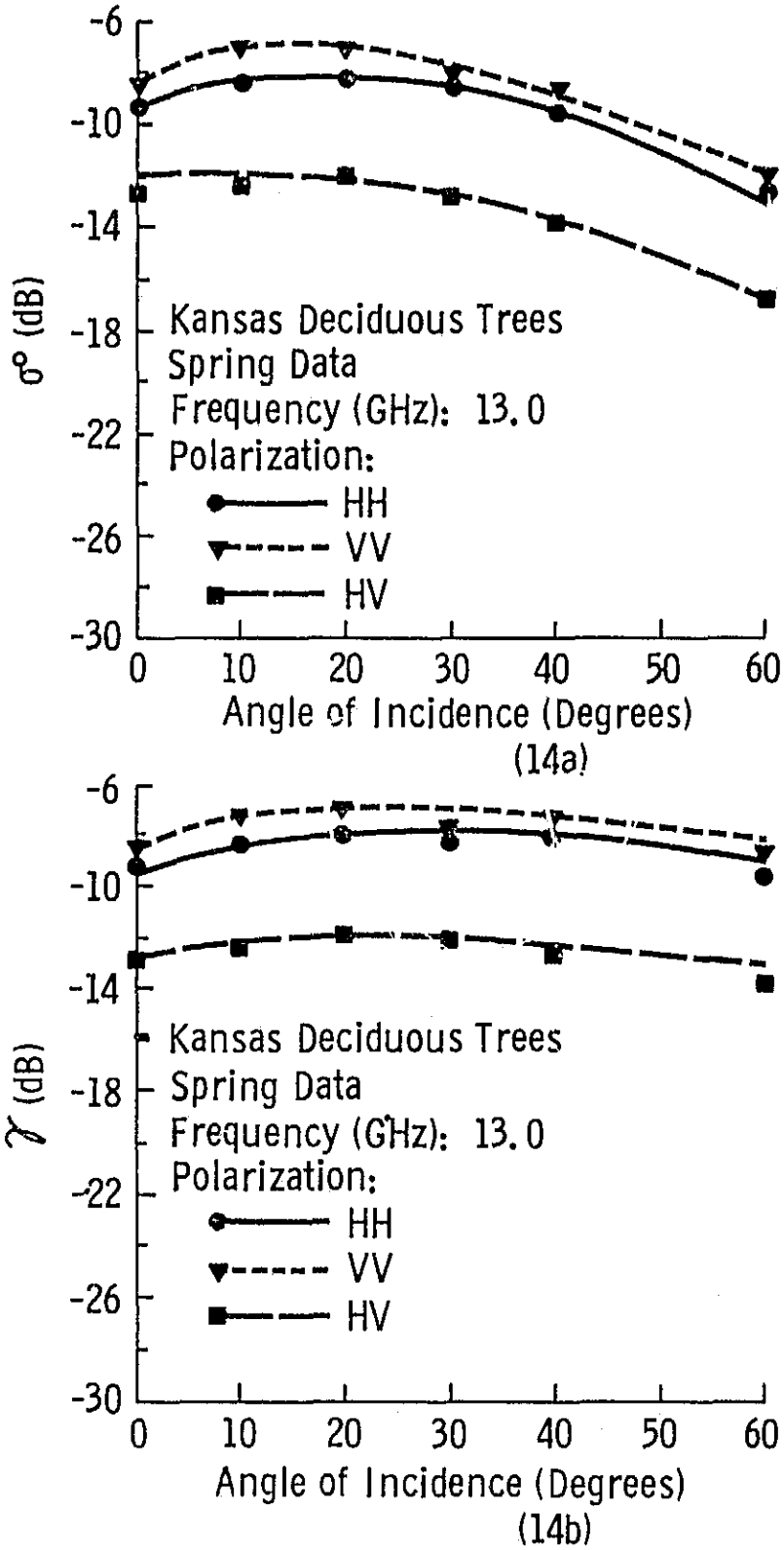

Figure 14. Angular Variations of $\overline{\sigma_H}^\circ$, $\overline{\sigma_V}^\circ$, and $\overline{\sigma_C}^\circ$ (14a) and γ_H, γ_V, and γ_C (14b) as Measured at 13.0 GHz. The Data Depicted in This Figure Were Gathered in the Springtime.

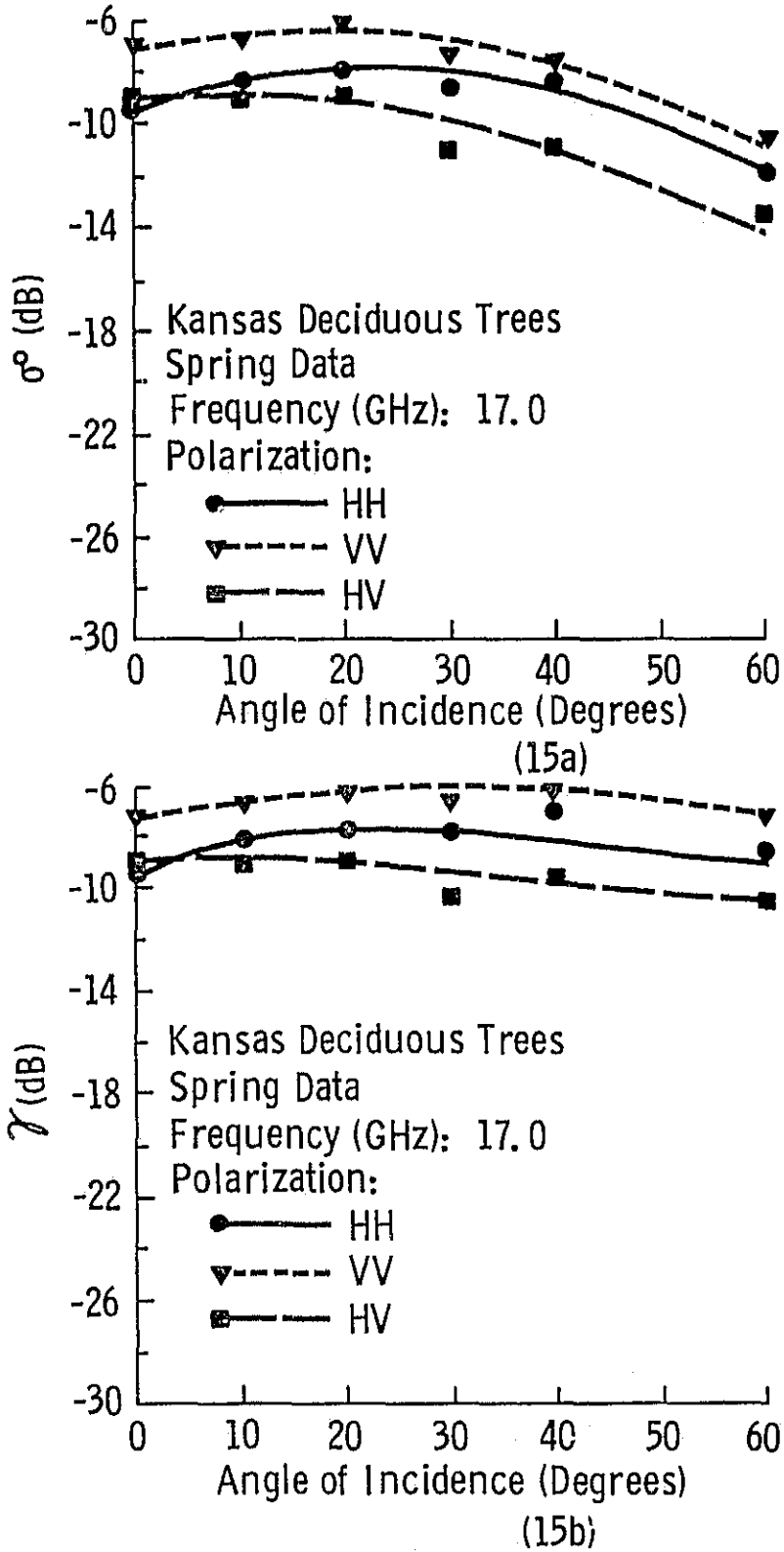

Figure 15. Angular Variations of $\overline{\sigma_H}^{\circ}$, $\overline{\sigma_V}^{\circ}$, and $\overline{\sigma_C}^{\circ}$ (15a) and γ_H, γ_V, and γ_C (15b) as Measured at 17.0 GHz. The Data Depicted in This Figure Were Gathered in the Springtime.

It is interesting to compare the data of Reitz [7] to those contained in this report. Operating an X-band (9.375 GHz) horizontally polarized side looking radar, data were collected over a variety of terrain types. One target studied was forest (New Jersey) land consisting of oak and pine trees. Figure 16 presents a comparison of Reitz's data with data collected with the MAS 8-18. Note that the data show very good agreement both in magnitude and in terms of their angular variations. Figures 17a-c present horizontally polarized data collected by Ament, MacDonald and Shewbridge of the Naval Research Laboratory [8]. Again the target was New Jersey forest lands. Data were gathered at 0.45, 1.25, 3.30 and 9.30 GHz with a multipolarized, forward looking pulsed radar. While neither the L-band (Figure 17a) nor the K-band (Figure 17c) data collected by NRL and KU show any significant agreement, the S-band (Figure 17b) data show similarities both in terms of magnitude (excepting nadir data) and angular trend. In Figure 18 further data are presented. These data were collected by Edison, Moore and Warner [9] using a near nadir looking pulsed radar over Pine Island, Minnesota. These data suggest the target to be nearly isotropic over the angular region shown with a magnitude of about 0 dB. This is not in agreement with the KU data which indicate not only a large discrepancy in the magnitude of σ°, with the KU data being an order of magnitude less, but also the shapes of the curves indicate the targets were of quite different character.

5.0 CONCLUDING REMARKS

An experiment has been performed to study the 1 to 18 GHz scattering behavior of deciduous trees. The results of this experiment have led to the following observations:

a) Data collected in the springtime indicate that σ° as measured between 1 and 18 GHz is an increasing function of frequency. Data collected in the fall do not, in general, show an increasing trend with frequency (8-18 GHz) and in some cases even shows a slight decrease as frequency increases.

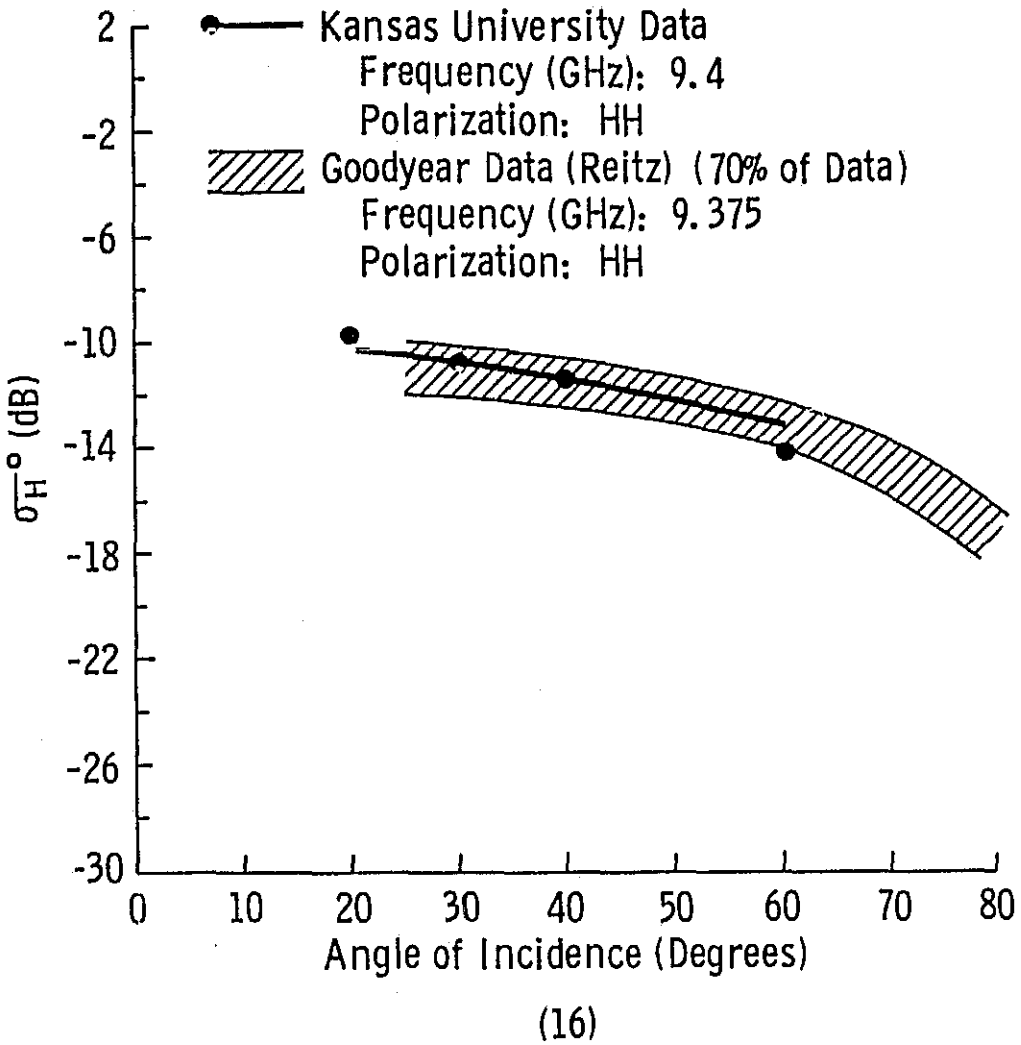

(16)

Figure 16. Angular Variations of $\overline{\sigma_H}^\circ$ as Measured by the Kansas University Scatterometer and $\overline{\sigma_H}^\circ$ as Measured with the Goodyear System. Note the Close Agreement of the Measurements.

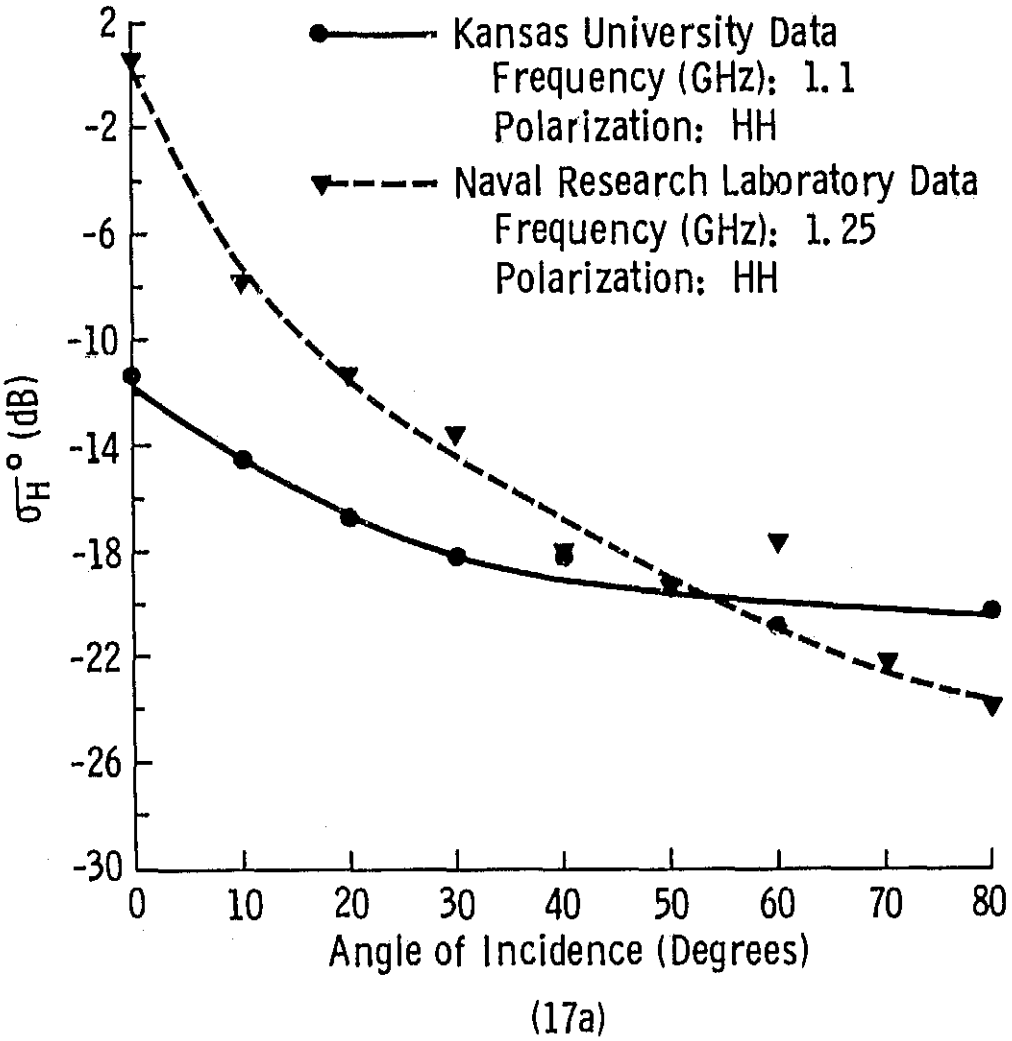

(17a)

Figure 17. Angular Variations of $\overline{\sigma_H}^\circ$ as Measured by the Kansas University System as Compared to $\overline{\sigma_H}^\circ$ as Measured by the NRL System. Data Are Presented at 1.1 GHz (17a), 3.3 GHz (17b), and 9.4 GHz (17c).

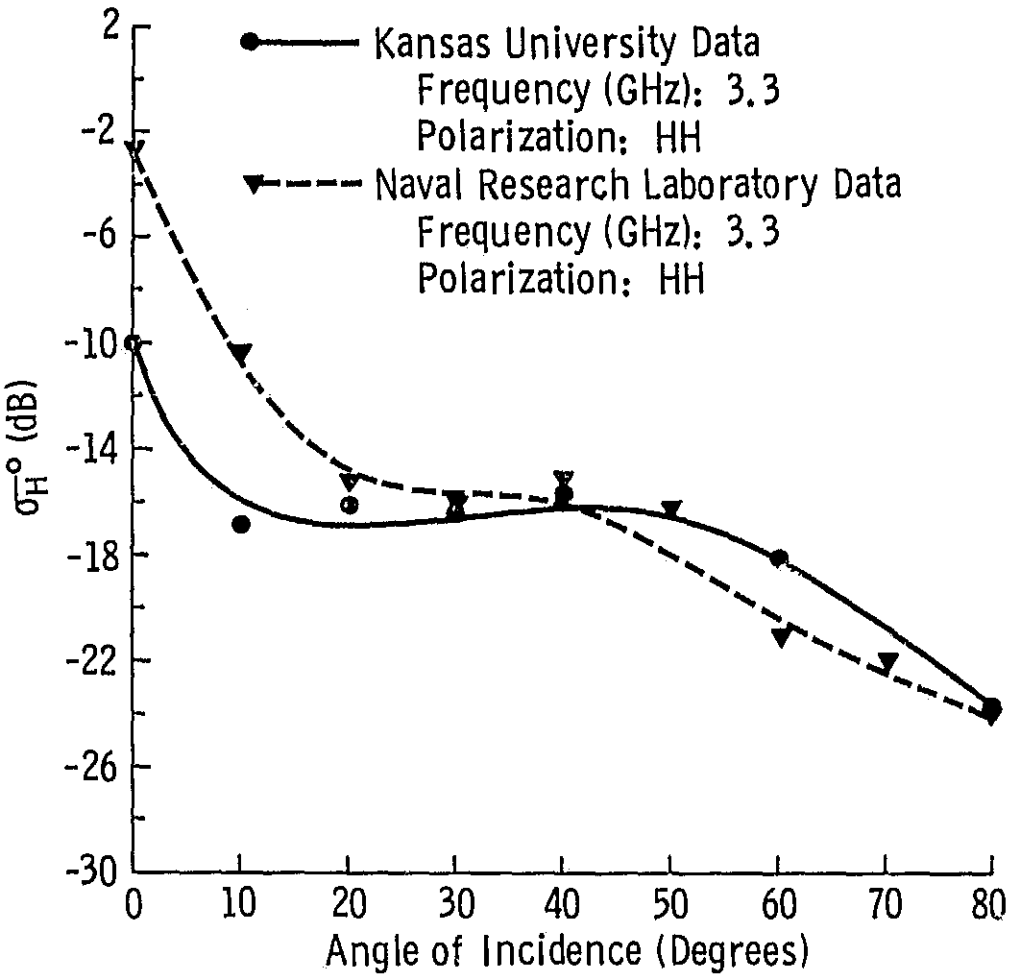
Kansas University Data
Frequency (GHz): 3.3
Polarization: HH
Naval Research Laboratory Data
Frequency (GHz): 3.3
Polarization: HH
σ_H° (dB)
2
-2
-6
-10
-14
-18
-22
-26
-30
0
10
20
30
40
50
60
70
80
Angle of Incidence (Degrees)

(17b)

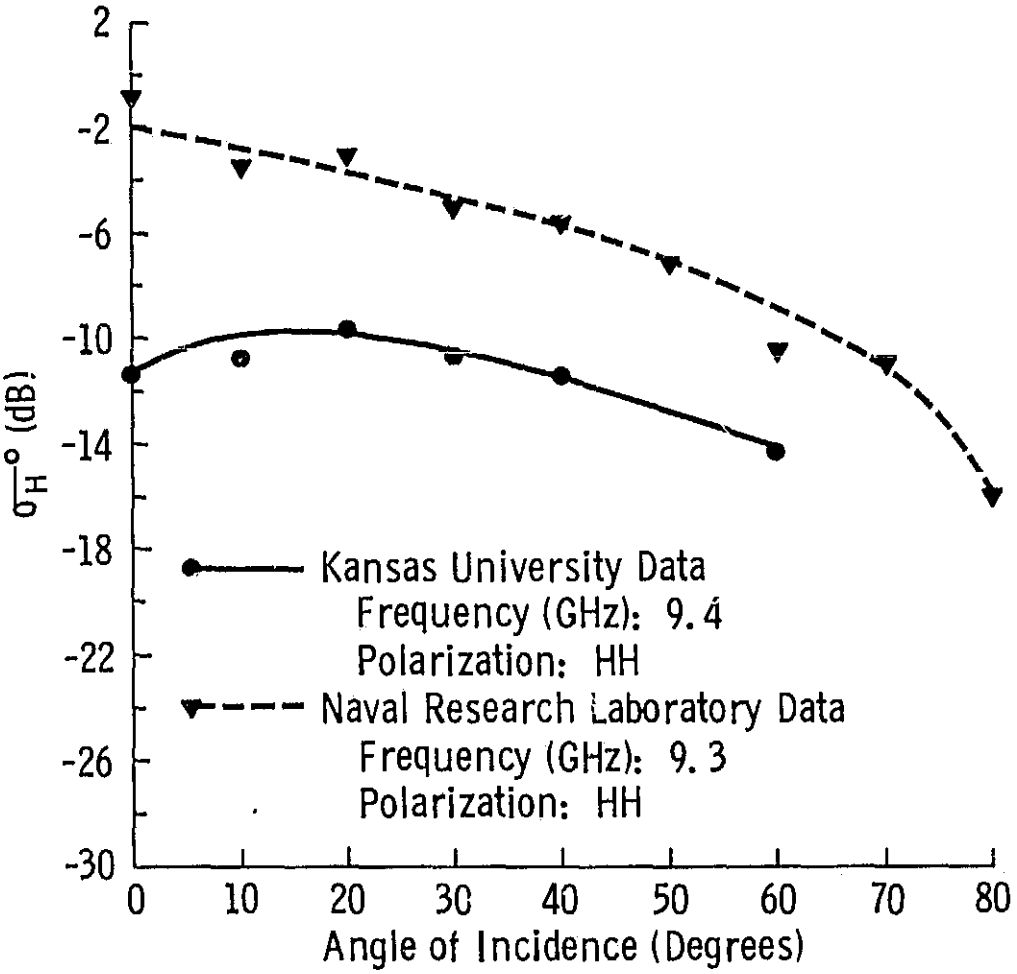
2
-2
-6
-10
-14
-18
-22
-26
-30
σ°_H (dB)
0
10
20
30
40
50
60
70
80
Angle of Incidence (Degrees)
Kansas University Data
Frequency (GHz): 9.4
Polarization: HH
Naval Research Laboratory Data
Frequency (GHz): 9.3
Polarization: HH

(17c)

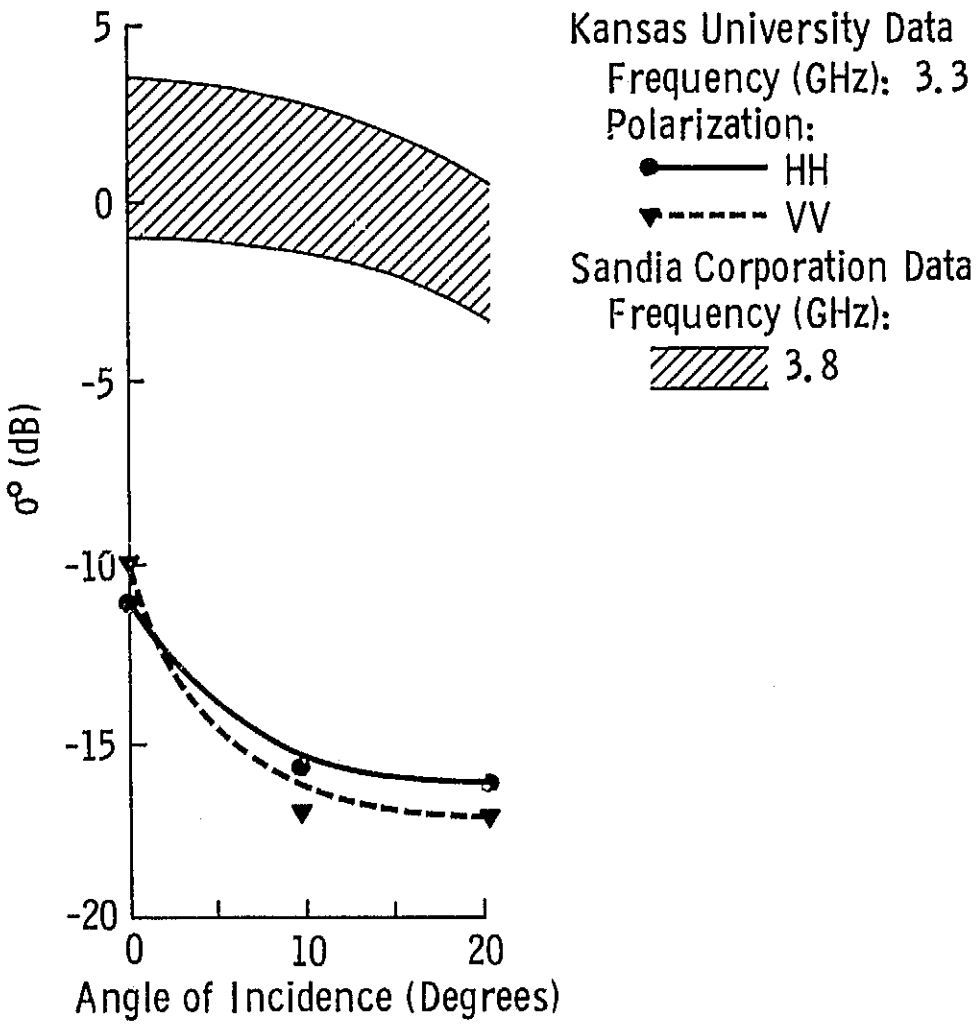

(18)

Figure 18. A Comparison of the Angular Variations of $\bar{\sigma}^{\circ}$ as Measured by Kansas University and by the Sandia Corporation. Note the Extreme Disparity Between the Two Data Sets.

b) The angular response to both spring and autumn data indicate that between about 7 and 18 GHz, volume scatter is the predominant scattering mechanism. Furthermore, cross polarized measurements, when available, substantiate this observation.

c) Data collected in the springtime are consistently higher in magnitude (as much as 11 dB) than those collected in the autumn. This effect is most apparent in the angle of incidence range between 30° and 50°.

d) A comparison of woodland data collected from various sources show that a wide range of scattering characteristics exists indicating that further measurements of forest lands is warranted.

REFERENCES

[1] Food and Agricultural Organization of the United Nations. World Forest Inventory. Rome, 1963.

[2] Avery, T. E., "Foresters Guide to Aerial Photo Interpretation," Agricultural Handbook 308, U. S. Department of Agriculture, Forest Service, 1966.

[3] Viskne, A. T., C. Liston and C. D. Sapp, "SLR Reconnaissance of Panama," Photogrammetric Engineering, v. 36, n. 3, pp. 253-259, March, 1970.

[4] Bush, T. F. and F. T. Ulaby, "8-18 GHz Radar Spectrometer," University of Kansas Center for Research, Inc., RSL Technical Report 177-43, Lawrence, Kansas, September, 1973.

[5] Oberg, J. M. and F. T. Ulaby, "MAS 2-8 Radar and Digital Control Unit," University of Kansas Center for Research, Inc., RSL Technical Report 177-37, Lawrence, Kansas, October, 1974.

[6] Bush, T. F. and F. T. Ulaby, "Fading Characteristics of Radar Backscatter from Selected Agricultural Targets," IEEE Trans. on Geoscience Electronics, v. GE-13, n.4, pp. 149-157, October, 1975.

[7] Reitz, E. A., "Radar Terrain Return Study, Final Report: Measurements of Terrain Backscattering Coefficients with an Airborne X-band Radar," Goodyear Aerospace Corporation Report, GERA-463, 1959.

[8] Ament, W., F. MacDonald and R. Shewbridge, "Radar Terrain Reflections for Several Polarizations and Frequencies," Trans. 1959 Symposium on Radar Return, Pt. 2, May 11-12, 1959, University of New Mexico N.O.T.S. TP 2339, U.S.Naval Ordnance Test Station, China Lake, California.

[9] Edison, A. R., R. K. Moore and B. D. Warner, "Radar Terrain Return at Near-Vertical Incidence," IRE Trans. on Antennas and Propgation, v. AP-8, pp. 246-254, May, 1960.